

The University of Maine

DigitalCommons@UMaine

Honors College

Spring 5-2018

Identification of TNFAIP8L1 Binding Partners Through Co-Immunoprecipitation and Mass Spectrometry

Audrey Hoyle

University of Maine

Follow this and additional works at: <https://digitalcommons.library.umaine.edu/honors>



Part of the [Biochemistry Commons](#), and the [Microbiology Commons](#)

Recommended Citation

Hoyle, Audrey, "Identification of TNFAIP8L1 Binding Partners Through Co-Immunoprecipitation and Mass Spectrometry" (2018). *Honors College*. 335.

<https://digitalcommons.library.umaine.edu/honors/335>

This Honors Thesis is brought to you for free and open access by DigitalCommons@UMaine. It has been accepted for inclusion in Honors College by an authorized administrator of DigitalCommons@UMaine. For more information, please contact um.library.technical.services@maine.edu.

IDENTIFICATION OF TNFAIP8L1 BINDING PARTNERS THROUGH CO-
IMMUNOPRECIPITATION AND MASS SPECTROMETRY

by

Audrey Hoyle

A Thesis Submitted in Partial Fulfillment
of the Requirements for a Degree with Honors
(Biochemistry and Microbiology)

The Honors College

University of Maine

May 2018

Advisory Committee:

Con Sullivan, Ph.D., Assistant Research Professor (Advisor)

Benjamin L. King, Ph.D., Assistant Professor of Bioinformatics

Melissa S. Maginnis, Ph.D., Assistant Professor of Microbiology

Sally Molloy, Ph.D., Assistant Professor of Genomics

Mary S. Tyler, Ph.D., Professor of Zoology

©2018 Audrey Hoyle

All Rights Reserved

ABSTRACT

The expanded understanding of the gene families and mechanisms governing tumorigenesis pathways has enormous potential for improving current cancer therapies and patient prognoses. One such gene family that participates in the regulation of tumorigenesis is the *tumor necrosis factor alpha-induced protein 8 (TNFAIP8)* gene family, which is comprised of four members: *TNFAIP8*, *TNFAIP8L1*, *TNFAIP8L2*, and *TNFAIP8L3*. The *TNFAIP8L1* gene is thought to function as a tumor suppressor, but the mechanisms by which it exerts this function have yet to be elucidated. We hypothesize that the TNFAIP8L1 protein acts as a tumor suppressor through protein-protein interactions that regulate tumor proliferation, migration, and/or angiogenesis. The H1299 non-small cell lung cancer cell line was engineered to overexpress TNFAIP8L1 protein and is being used as an *in vitro* model to identify putative protein binding partners through co-immunoprecipitation and mass spectrometry assays. Apparent interactions will be validated by mammalian two-hybrid assays. We anticipated that TNFAIP8L1 would bind proteins involved in tumorigenesis pathways and that these may reveal new avenues of study and hold important clinical relevance in current cancer treatment plans. We identified 138 putative protein interactions involving TNFAIP8L1.

“Don't you know
They're talking about a revolution
It sounds like a whisper
And finally the tables are starting to turn
Talking about a revolution
Yes, finally the tables are starting to turn”
– Tracy Chapman

To everyone who is fighting to turn the tables.

ACKNOWLEDGEMENTS

I would like to thank all of the people whom I have crossed paths with that have changed my life for the better. Firstly, I would like to express my sincere gratitude to my advisor, Dr. Con Sullivan, who patiently guided me and taught me every single day in the lab and offered me life advice along the way. Without his knowledge, patience, and kindness none of this would have been possible. Next, I would like to thank the members of my committee whom continually provided their support and advice without any reservations. You have helped me tremendously. To Sari, you have made my experience in lab an absolute joy and I am better as a scientist and as a person for knowing you. To the other faculty, graduate students and undergraduate students that have given me their understanding, kindness and much laughter during my time here, I am forever grateful. Finally, thank you to my parents and siblings who have given me unwavering support, love and guidance throughout my life. I love you.

Research reported in this project was supported by an Institutional Development Award (IDeA) from the National Institute of General Medical Sciences of the National Institutes of Health under grant number P20GM103423. Additionally, this project was financially sponsored by the INBRE- Honors College Comparative Functional Genomics Thesis Fellowship.

TABLE OF CONTENTS

INTRODUCTION	1
Overview	1
Cancer	4
Lung Cancer	7
H1299 Cell Line	9
<i>TNFAIP8</i> Gene Family	11
<i>TNFAIP8</i>	12
<i>TNFAIP8L1</i>	13
<i>TNFAIP8L2</i>	14
<i>TNFAIP8L3</i>	15
Interactomics	16
Mass Spectrometry	17
MATERIALS AND METHODS	19
RESULTS	28
DISCUSSION	38
REFERENCES	42
APPENDIX A	47
Supplementary Data	47
AUTHOR'S BIOGRAPHY	55

LIST OF FIGURES

Figure 1: Hallmarks of Cancer	3
Figure 2: Top 10 Types of Cancer	8
Figure 3: Proposed Mechanism of <i>TNFAIP8</i> Variant 2	12
Figure 4: Comparison of amino acid sequences among the <i>TNFAIP8</i> gene family	14
Figure 5: Structure of TNFAIP8L2	15
Figure 6: Co-Immunoprecipitation Schematic	22
Figure 7: Mammalian Two-Hybrid Assay Schematic	27
Figure 8: Western Blot Results	29
Figure 9: REVERT™ Total Protein Stain Results	30
Figure 10: Venn Diagram of Protein Interactors	32
Figure 11: Biological Processes of TNFAIP8L1 Interactors	34
Figure 12: Web of associated Protein Interactions	35-36
Figure 13: Mammalian Two-Hybrid Assay Results	37
Supplementary Figure 1: Additional Mammalian Two-Hybrid Results	47

LIST OF TABLES

Table 1: Cancers Associated with TNFAIP8 Gene Family	4
Table 2: Interactomics Techniques Summary	17
Table 3: Mass Spectrometry - Mass Analyzers Comparison	18
Table 4: Polymerase Chain Reaction (PCR) Primers	24
Table 5: Mammalian Two-Hybrid Fusion Constructs	25
Table 6: Putative Interactors Gene Summary	33
Supplementary Table 1: Putative Interactors Extended Summary	48-54

INTRODUCTION

Overview

Cancer is a devastating disease and one of the most clinically relevant illnesses of our time. It was the second leading cause of death worldwide in 2015, claiming the lives of 8.8 million people (World Health Organization, 2018). There are many burdens associated with cancer to the individual, health care systems, and society at-large. Approximately 40% of people will be diagnosed with cancer in their lifetime, resulting in 171.2 deaths per 100,000 people each year (World Health Organization, 2018). The leading cause of cancer deaths is lung cancer, which accounts for 25% of all cancer deaths. This is more than colon, breast, and prostate cancer combined (American Cancer Society, 2018). Despite these overwhelming statistics, there is no cure for cancer.

There are numerous clinical approaches to treat cancer, but they are not flawless and leave room for improvement. In the 1960's cancer treatments and therapies were beginning to be researched and integrative approaches were implemented. During the period from 1974 to 1976, the 5-year relative survival rate for all cancers combined was 50% for adults and 62% for children (National Institute of Health, 2013). Current techniques combine elements of medicine and lifestyle changes. A few of the most common medical interventions are chemotherapy, radiotherapy, and surgery. Chemotherapy uses drugs to kill cancer cells, usually through pills, intravenous access, or injection. It is commonly used in conjunction with other therapies like radiotherapy or surgery. Radiotherapy uses high doses of radiation to kill cancer and shrink tumors (National Cancer Institute, 2017). With the advances in technology, and evidence-based

research, there has been an increase in survival rates for adults and children diagnosed with cancer. As of 2006, the 5-year survival rates of adults and children diagnosed with cancer had increased to 68% and 81%, respectively (National Institute of Health, 2013).

As improved understanding of the mechanisms behind tumorigenesis and technological advances occur, the survival numbers should continue to increase. The importance of regular physician visits for screening, diagnosis, therapies, and treatment are crucial, but it is beneficial to also consider the importance of prevention. Important factors for prevention include diet choice, exercise, and environmental exposure to carcinogens. In regard to diet, the American Cancer Society recommends that the amount of red meat and processed meat ingested, as well as the number of alcoholic beverages consumed, be limited. It is also beneficial to eat adequate amounts of fruits and vegetables, as well as switching from refined to whole grains. Adults should engage in moderate intensity physical activity for at least 2.5 hrs per week, and children should get 1 hr of moderate intensity physical activity per day (American Cancer Society, 2016). Other things to consider are vaccinations against oncogenic viruses like human papillomavirus, as well as limiting exposure to cigarette smoke and ultraviolet radiation (Center for Disease Control and Prevention, 2018).

There are numerous causes of cancer, but most exhibit these six hallmarks of acquired biological capabilities: evading apoptosis, self-sufficiency in growth signals, insensitivity to anti-growth signals, sustained angiogenesis, limitless replicative potential, and the ability to invade tissues and metastasize (**Figure 1**) (D Hanahan & Weinberg, 2000). Though this view reduces a complex group of diseases down to a few common features, it can be helpful to initially study cellular processes in a microcosm. However, it

should also be mentioned that a systems biology approach would be beneficial to understanding disease processes since the processes in nature do not exist in a microcosm (Fang & Casadevall, 2011).

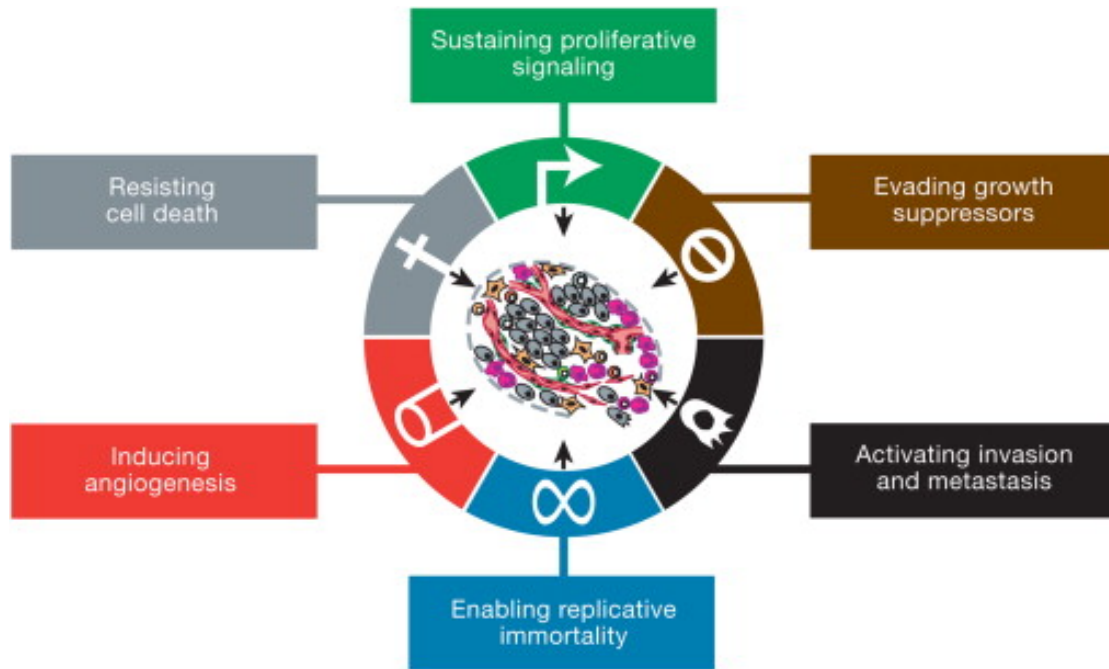


Figure 1. The six hallmarks of cancer shown as acquired capabilities of cells (Douglas Hanahan & Weinberg, 2011). Cell, Volume 144, Issue 5, Douglas Hanahan, Robert A. Weinberg, Hallmarks of Cancer: The Next Generation, Pages 646-672, Copyright (2011), with permission (4339050057477) from Elsevier.

Regulation of these processes occurs through many different gene families and proteins at work, including the *tumor necrosis factor alpha-induced protein 8* (*TNFAIP8*) gene family, a relatively new, yet significant family in the regulation of inflammation, immunity, and cancer processes (Lou & Liu, 2011). The *TNFAIP8* gene family is comprised of four members: *TNFAIP8*, *TNFAIP8L1*, *TNFAIP8L2*, and *TNFAIP8L3* (Sullivan, Lage, Yoder, Postlethwait, & Kim, 2017). All four gene family members encode for proteins that are thought to contain seven alpha helices, with a hydrophobic cavity in the center. The cavity is thought to serve as a binding site for co-factors and molecules interacting with the protein, including lipid second messengers

required for signaling (Fayngerts et al., 2014; X. Zhang et al., 2009). *TNFAIP8* and *TNFAIP8L2* are involved with immune regulation and inflammation, as well as the development and regulation of cancers through roles as either tumor suppressors or tumor promoters (Porturas et al., 2015; X. Zhang et al., 2009). The entire *TNFAIP8* gene family has been linked to cancers ranging from liver and lung cancer to blood and bone cancers (**Table 1**). The *TNFAIP8L1* gene is thought to function as a tumor suppressor, but the mechanisms by which it exerts this function have yet to be elucidated, leaving potential for improving current cancer therapies and patient prognoses with increased understanding of the mechanisms (Z. Zhang et al., 2015) .

Gene	Function	Associated Cancers	References
<i>TNFAIP8</i>	Tumor Promoter or Tumor Suppressor	Stomach, Prostate, Ovarian, Lung , Blood, Bone	(Chen et al., 2016; Cheng et al., 2015; Eisele et al., 2007; Liu et al., 2012; Xing & Ren, 2016)
<i>TNFAIP8L1</i>	Tumor Suppressor	Liver, Lung	(Wu et al., 2017; Z. Zhang et al., 2015)
<i>TNFAIP8L2</i>	Tumor Suppressor	Stomach, Kidney, Liver, Lung , Bone	(Cao et al., 2013; Deng, Feng, & Deng, 2015; Y. Li et al., 2015; Peng et al., 2016; Zongliang Zhang, Qi, Hou, & Jin, 2013)
<i>TNFAIP8L3</i>	Tumor Promoter	Lung , Cervix, Colon	(Fayngerts et al., 2014b)

Table 1. Cancer types previously associated with each gene in the *TNFAIP8* gene family.

Cancer

Cancer is a group of diseases where cells in the body divide uncontrollably and migrate into surrounding tissues (National Cancer Institute, 2015). It is characterized by the six hallmarks of cancer (**Figure 1**)(D Hanahan & Weinberg, 2000). Cancer is a

disease that arises from changes in genes that control cellular functions such as the cell cycle, cell metabolism and cell death. These genetic changes can occur due to many environmental and lifestyle factors, as well as a number of unknown reasons. Behaviors such as tobacco smoking, use of drugs and alcohol, as well as ultraviolet, and x-ray radiation can increase the risk of cancer (National Cancer Institute, 2015). According to the World Health Organization, dietary choices, including processed meat and red meat, can also cause increased risks of cancer, especially colorectal cancer (Harvard School of Public Health, 2015).

There are more than 100 types of cancer, ranging from the more common breast, prostate, and lung cancers to more rare types such as fallopian tube or heart cancer (National Cancer Institute, 2015). Cancer has a massive impact on individuals, families, and societies across the globe. In 2012, there were 14 million new cases of cancer and 8.2 million cancer related deaths. In the United States alone, 1.68 million new cases of cancer were estimated for 2016 (“Cancer Statistics - National Cancer Institute,” 2017). These statistics place cancer as the second leading cause of death globally and there is currently no cure, however, there are numerous treatment options with varying degrees of success depending on cancer type (World Health Organization, 2018).

The devastation that cancer leaves in its wake is shown in the statistics above, but it also takes a toll on the economy of nations, the health care system, and survivors. It is estimated that the direct health care costs in the United States for cancer in 2015 reached 80.2 billion USD and the total economic cost including loss of productivity was 1.16 trillion USD in 2010 (American Cancer Society, World Health Organization 2018). With the number of cases predicted to rise, the economic costs will also rise. The personal and

societal problems associated with cancer are demonstrated in quality of life research performed with the help of survivors. One study revealed that there were four major domains of life that were altered for survivors including physical well-being, psychological well-being, social well-being and spiritual well-being (Mollica, Nemeth, Newman, & Mueller, 2015). The survivors noted decreased satisfaction in these areas of their life. Physical well-being was marked by dissatisfaction in strength, fatigue pain, and the ability to perform daily activities, while psychological well-being was marked by issues of anxiety, depression, and fear of recurrence of cancer. The last two domains focused on issues relating to hope, inner strength, religion, appearance, relationships, and feelings of isolation (Mollica et al., 2015). As scientists, citizens, and humans, there should be an emphasis placed on filling knowledge gaps surrounding cancer processes and their regulations so that more effective prevention and treatment options can be revealed.

It is also important to note that a disproportionately high number of cancer cases due to preventable diseases such as human papillomavirus and cancer deaths occur in low-income and middle-income countries, where prevention, diagnosis and treatment are not affordable or available (World Health Organization, 2018). The best way to reduce the burden of cancer is to avoid risk factors, vaccinate against cancer associated viruses, and get regular screenings. Prevention and early detection are vital to decreasing cancer burden (American Cancer Society, 2018a). There are several clinical approaches to treat cancer, but they are not perfect and leave room for improvement in patient outcomes, cost effectiveness, and specificity of treatment as outlined previously. There is a promising new approach for treatment that relies on individual genomic differences termed

personalized medicine. The idea is that each person's disease has a unique susceptibility based on their "genomic blueprint" ("Personalized Medicine,"). It is essential that research continues into the mechanisms regulating tumorigenesis and specifically, it is important to gain a better understanding of gene families such as the *TNFAIP8* gene family because they provide greater insight into the mechanisms that govern tumorigenesis. Other priorities include increasing political commitment to cancer prevention, monitoring cases and costs, as well as developing standard tools and treatment methods (World Health Organization, 2018).

Lung Cancer

Cancers that form in tissues of one or both lungs, usually in the cells that line airways, are referred to as lung cancer. Lung cancer begins when cells of the lung(s) begin to grow and divide abnormally, allowing them to form tumors and spread to other areas of the body (American Cancer Society, 2018a, 2018b). There are two major forms of lung cancer, non-small cell lung cancer and small cell lung cancer. Non-small cell lung cancer makes up 80-85% of all lung cancers, with the other 10-15% being small cell lung cancers. Lung cancers are the second most common cancer in men and women, excluding skin cancer, (American Cancer Society, 2018b) and are the leading cause of cancer deaths in males and females in the United States (**Figure 2**).

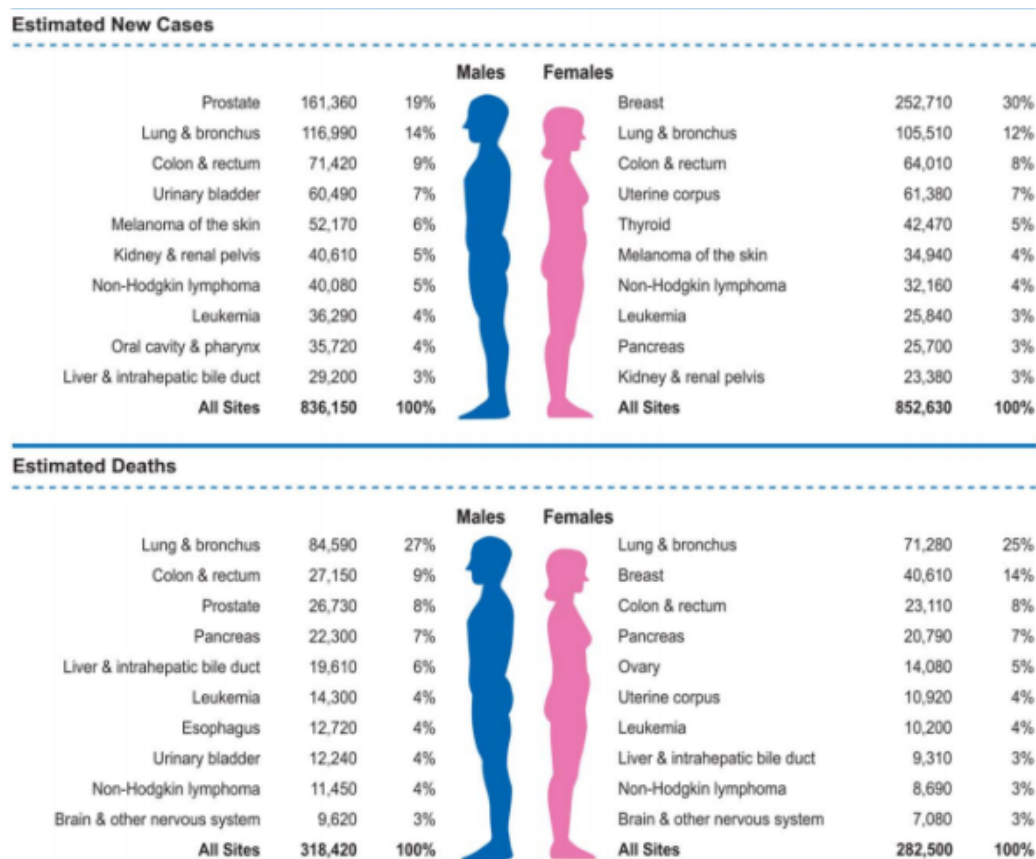


Figure 2. Top ten cancer types in males and females in 2017 in the United States. Top shows estimated new cases and bottom shows estimated deaths. Lung cancer is leading in cancer deaths among both sexes. (Siegel et al., 2017). Copyright © 2017, John Wiley and Sons. Reprinted by permission from John Wiley and Sons (4339050472934). Cancer Journal for Clinicians. Siegel, R. L., Miller, K. D., & Jemal, A. (2017). Cancer statistics, 2017. *CA: A Cancer Journal for Clinicians*, 67(1), 7–30. <https://doi.org/10.3322/caac.21387>

Smoking cigarettes is the number one risk factor for developing lung cancer and is linked to 80-90% of all lung cancers. Smoking increases the risk of developing lung cancer by 15 to 30 times. Second-hand smoke is also linked to an increased risk of development of lung cancer, especially when children are between the ages of 3-11 years old (Center for Disease Control and Prevention, 2017). While the survival rates for most cancer diagnoses have increased, lung cancer mortality rates remain high. The 5-year survival rate for lung cancer is 18%, which is partially attributable to the fact that most

cases are caught in late stages. Over 50% of cases are diagnosed at a stage where treatment is rarely effective. Of lung cancer cases diagnosed in late stages, only 4% of patients live for more than 5 years (Siegel, Miller, & Jemal, 2017). This demonstrates the need for new and more effective prevention, detection, and treatment protocols.

Mammalian Cell Culture and NCI-H1299 Cells as Model

The NCI-H1299 (H1299) cell line is derived from the lymph node metastasis of a non-small cell lung carcinoma in a 43-year-old Caucasian male. The cells do not express p53 protein, a known tumor suppressor, due to a homozygous partial deletion. They do have the ability to produce neuromedin B, but not gastrin releasing peptide. Both neuromedin B and gastrin releasing peptides are the mammalian homologs of bombesin, which is a protein used as a tumor marker in small cell lung cancer and stomach cancer among others (American Type Culture Collection, 2016; Wang, Knezetic, Schally, Pour, & Adrian, 1996). H1299 cells are adherent epithelial cells that can be used as a mammalian cell culture model and are suitable for transfections (American Type Culture Collection, 2016).

Cell culture can be used as an *in vitro* or *in vivo* model, but is generally used in two-dimensional (2D) cell culture as an *in vitro* model. To be used as an *in vivo* model, H1299 cells are typically transplanted into recipient animal models such as mice. These xenotransplantation models are often used as an initial step in research to understand how cancer cells of various types behave in a live organism (Giovanella, Yim, Stehlin, & Williams, 1972). A possible bridge between 2D *in vitro* studies and *in vivo* studies are those of three-dimensional (3D) cell culture. In typical 2D cell culture, cells are cultured on flat plastic flasks, or dishes in medium suited for the particular cells to grow in. The

cells are then grown in a monolayer and passaged, until used for further experimentation. This method has benefits of being fast, easy, and cost-effective; however, it also has its drawbacks. Cells grown in 2D culture exist in a monolayer composed of growing and dividing cells, where all dead cells have detached from the culture vessel. The dead cells are then removed with each passaging. Also, cells grown in 2D models are more stretched out and flat than they normally grow leading to an abnormal cell morphology. This abnormal morphology could have influences over processes of interest such as cell proliferation, gene expression, and protein expression. Overall, these cells may not behave as they would in vivo (Edmondson, Broglie, Adcock, & Yang, 2014). On the other hand, 3D cell culture is becoming more popular as it has all the benefits of 2D cell culture and being an in vitro model, however it better mimics the microenvironments of in vivo studies. The cells are cultured using hydrogel or an agar layer to allow cells to grow in all directions. This model allows cells to interact with each other in a way more accurate to in a live model. It is important to note that the 3D system also has drawbacks in the ways that you have cells growing together, but they do not possess vascular systems so the passage of waste, nutrients, and oxygen are only carried out by diffusion. This limits the size of spheroids that can be grown and what types of cells can be used (Edmondson et al., 2014).

Overall, cell culture allows the cells removed from various animal or plant tissues to be grown in artificial media. After cells are isolated and grown up on artificial media to a point where they must be passaged, they become cell lines. Cell lines are immortalized through acquisition of genetic mutations that allow them to grow and these cell lines can then be continually passaged and used in research. The culture conditions

for each cell type vary, but they all require essential nutrients such as amino acids, carbohydrates, and gas exchange. Cell culture is one of the most important tools available to study biochemical processes and allows for results to be consistent and reproducible (*Cell Culture Basics Handbook*, 2016). It also provides the advantage of being relatively easy, and cost effective.

In this study, the H1299 cell line was used as a 2D model, where a monolayer of cells is grown in a tissue culture flask or dish and then passaged for continuation of the cell line.

TNFAIP8 Gene Family

The *tumor necrosis factor-alpha-induced protein 8 (TNFAIP8)* gene family is a recently discovered family that has been found to be involved in regulation of tumorigenesis, inflammation, and immunity (Lou & Liu, 2011). The four members *TNFAIP8*, *TNFAIP8L1*, *TNFAIP8L2*, and *TNFAIP8L3* all encode for proteins with a unique structure that includes seven alpha helices surrounding a central hydrophobic cavity (Sullivan et al., 2017). The gene family members *TNFAIP8* and *TNFAIP8L2* are activated by TNF- α in times of environmental stress. Since discovery of this gene family, there have been many studies to elucidate structure and function of the members, however *TNFAIP8L1* still remains uncharacterized. *TNFAIP8* functions as a tumor promoter or tumor suppressor, depending on the splicing variant (Lowe et al., 2017) and has been associated with lung, blood and bone cancers among others. *TNFAIP8L1* functions as a tumor suppressor and has been linked to liver and lung cancer, but the mechanism by which it exerts this function has yet to be elucidated. *TNFAIP8L2* is also classified as a tumor suppressor and has also been linked to liver and lung cancer. The

last member, *TNFAIP8L3*, has been shown to function as a tumor promoter and is associated with lung, cervix, and colon cancers (**Table 1**).

TNFAIP8

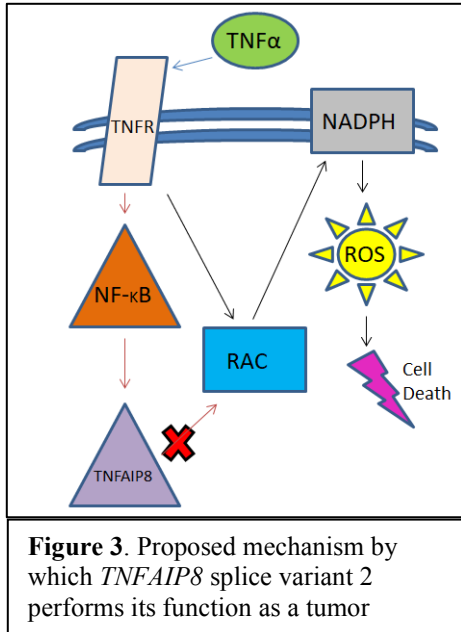


Figure 3. Proposed mechanism by which *TNFAIP8* splice variant 2 performs its function as a tumor

TNFAIP8, also known as SSC-S2, GG2-1, and MDC-3.13, is an oncogenic protein and apoptotic regulator (X. Zhang et al., 2009). It was the first gene family member described and is one of the most well characterized genes in the family along with *TNFAIP8L2*. It has been shown to act as either a tumor promotor or tumor suppressor depending on the splice variant and cell type affected (Kumar et al., 2004; Lowe et al., 2017).

One study showed that variant 2 is overexpressed in many human cancers including lung adenocarcinoma, lung squamous cell carcinoma, and hepatocellular carcinoma, where variant 1 of *TNFAIP8* is downregulated and variants 3,4,5 and 6 are expressed at very low levels (Lowe et al., 2017). The proposed mechanism by which variant 2 promotes cancer is through p53 repression, in effect cancelling out its ability to induce apoptosis and inhibit tumorigenesis. *TNFAIP8* has also been hypothesized to protect cells against apoptosis through inhibiting Rac1 (**Figure 3**). The TNF-α cytokine activates the tumor necrosis factor receptor (TNFR), which activates Rac1 and NF-κB. Rac1 is responsible for promoting cell death through the ultimate promotion of reactive oxygen species (ROS), but the TNFR also activates NF-κB which increases *TNFAIP8* expression

allowing it to inhibit Rac1 and therefore stopping the production of ROS and cell death (Porturas et al., 2015).

TNFAIP8L1

TNFAIP8L1 is expressed in many tissues, and a study in mice revealed that TNFAIP8L1 was found in tissues ranging from neurons in the brain, muscle tissue, and hepatocytes, as well as many cells of epithelial origin. This is important because epithelial tissues play a role in many processes such as absorption, secretion, and immunity (Cui et al., 2011). TNFAIP8L1 was shown to induce apoptosis in hepatocellular carcinoma cells (HCC) by negatively regulating Rac1 and altering down-stream pathway activations (Z. Zhang et al., 2015). This is comparable to the proposed mechanism by which TNFAIP8 carries out its functions. *TNFAIP8L1* has also been shown to inhibit the growth of lung cancer, with low levels expressed in tumor tissue (Wu et al., 2017). Decreased levels of *TNFAIP8L1* have been correlated with poor patient survival and have led to the hypothesis that it can be used as a negative prognostic indicator for lung cancer patients (Wu et al., 2017). To fully understand the function of TNFAIP8L1, we must understand the structure. It is hypothesized that the structure of TNFAIP8L1 is very similar to TNFAIP8L2, which is composed of 7 anti-parallel alpha helices. There is also a central hydrophobic cavity which is a potential site for co-factor binding and may play a role in immune homeostasis (X. Zhang et al., 2009). Based on this known structure of TNFAIP8L2 and the comparison of each amino acid residue among the gene family members (**Figure 4,5**)(Sullivan et al., 2017), it is suggested that TNFAIP8L1 has a similar structure as described for TNFAIP8L2.

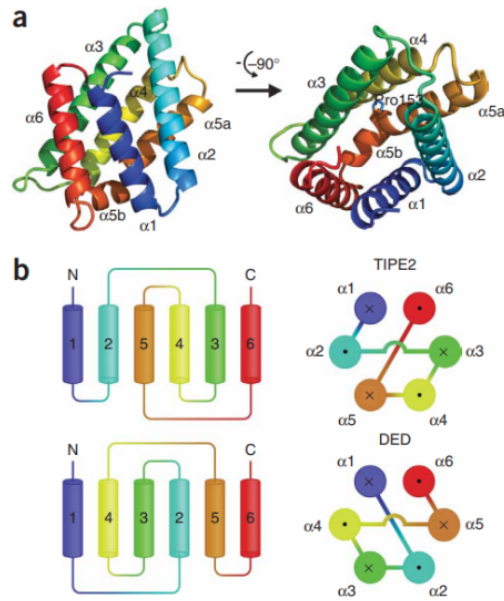


Figure 5. (a) The overall structure of TNFAIP8L2 showing all six alpha helices. (b) TNFAIP8L2 topology is different than that of the DED domain (X. Zhang et al., 2009). Reprinted by permission from Springer Nature: Zhang, X., Wang, J., Fan, C., Li, H., Sun, H., Gong, S., ... Shi, Y. (2009). Crystal structure of TIPE2 provides insights into immune homeostasis. *Nature Structural and Molecular Biology*, 16(1), 89–90. <https://doi.org/10.1038/nsmb.1522>

phosphoinositide second messenger binding (**Figure 5**) (Fayngerts et al., 2014b; X. Zhang et al., 2009).

TNFAIP8L2 plays an important role in immune homeostasis and has also been shown to inhibit human hepatocellular carcinoma metastasis in HCC-derived cells lines. A study

of 112 patients showed that loss or reduction of TNFAIP8L2 in primary HCC tissues led to greater metastasis. It was discovered that the cause is that

TNFAIP8L2 inhibits the migration and invasion of cancer cells through inhibition of Rac1 (Cao et al., 2013). This targeting of Rac1 is consistent with studies performed using TNFAIP8 and TNFAIPL1 and shows a similarity in execution of tumor suppression.

TNFAIP8L3

TNFAIP8L3 is a cytoplasmic protein that is expressed in various mouse and human tissues, but generally restricted to cell types of epithelial origin. High levels have been detected in the digestive tract, the islets of the pancreas, and breast duct epithelial cells (Cui et al., 2015). The protein expression similarities between human and mice may

be due to the homologous sequences they share and this trend of tissue specific expression has been shown in studies of other gene family members (Chen et al., 2016; Cui et al., 2011, 2015). TNFAIP8L3 has been shown to function as the transfer protein of phosphoinositide second messengers that promote cancer. Similar to the structure of TNFAIP2, it has a large hydrophobic cavity that can bind lipid second messengers (Fayngerts et al., 2014b). In human cancers associated with TNFAIP8L3 upregulation subsequent knockout of TNFAIP8L3 results in decreased tumorigenesis. Conversely in cell culture, when TNFAIP8L3 expression is forced, tumorigenic effects are increased (Fayngerts et al., 2014b).

Interactomics

Interactomics is the study of protein-protein interactions and their implications using scientific experimentation and bioinformatics for analysis. The study of protein interactions is necessary for understanding cellular function and more complex pathways where proteins are interacting (Dammeyer & Schobert, 2010). There are many different techniques for studying and/or validating these interactions including co-immunoprecipitation coupled with mass spectrometry, yeast two-hybrid assays, mammalian two-hybrid assays, proximity ligation assays, and bimolecular fluorescence complementation (**Table 2**).

Utilizing mass spectrometry based proteomics allows the protein itself to be used to isolate its binding partners. In the past, yeast two hybrids were used, but the advantages of co-immunoprecipitation with mass spectrometry analysis include that multi-component complexes can be isolated with only one step, and that it utilizes the protein of interest in its processed form (Free, Hazelwood, & Sibley, 2009). Data indicate

that mass spectrometry coupled with co-immunoprecipitation is a quick, safe, and efficient way of identifying protein-protein interactions. It is one of the best tools available for elucidating previously unknown protein partners due to the volume of data and interactors that can be processed (Moresco, Carvalho, & Yates, 2010).

Interactomics Technique	Advantages	Disadvantages
Co-immunoprecipitation and Mass Spectrometry	Isolation of protein complexes, protein of interest is in processed form, large scale, time effective	Not all interactors are true interactors, not able to resolve interactors in complexes, does not validate specific interactions
Mammalian Two-Hybrid Assay	Fast, inexpensive, flexibility of interactors	Direct interactors only, some proteins can be toxic to host cells
Yeast Two-Hybrid Assay	Eukaryotic form, can be scaled up easily	Direct interactors only, interacting proteins must move to the nucleus, proteins not in natural environment, issues with post translational modifications occurring properly
Proximity Ligation Assay	Easy, sensitive, can closely mimic natural environment for the protein	Direct interactors only, increased cost, increased time for result output
Bimolecular Fluorescence Complementation	Allows for tracking of interactions over time and changing conditions, sensitive, can detect direct and indirect interactors	Requires expensive equipment, not best choice for direct interactions

Table 2. Summary of the advantages and disadvantages of the major interactomics techniques used for studying and validating protein-protein interactions.

Mass Spectrometry

Mass Spectrometry is an analytical technique that separates ions based on their mass-to-charge ratio. Two particles with the same mass-to-charge ratio will separate in

the same way. The first step is ionization of the sample, where electrons are removed to give the sample a positive charge. Post ionization, the ions are accelerated to a uniform kinetic energy and subjected to a magnetic field. Deflection of the ions as they pass through the magnetic field will vary based on their size and charge, giving a mass-to-charge ratio. Smaller ions and ions with the greatest charge are deflected at a higher rate. The beam of ions passes through a detector that allows a spectral fingerprint to be recorded (Breci, 2017). The spectral data are reported as relative abundance versus mass-to-charge ratio. These are then entered into a spectral database for analysis and determination of protein identity (Cottrell, 2011).

Instrument	Advantages	Disadvantages
Quadrupole Mass Analyzer	Relatively cheap and fast, reproducible results	Lower resolving power,
Time of Flight Mass Analyzer	Fast, sensitive, increased molecular weight range-useful for biological samples	Limited dynamic range
Quadrupole Ion Trap Mass Analyzers	Qualitative work (i.e protein identification), sensitive, high resolution	Quantitative work, not optimal for work with masses below 100 Da, Low scan rate

Table 3. Advantages and disadvantages of widely used mass analyzers.

MATERIALS AND METHODS

Cell Culture

NCI-H1299 Cell Line was grown in Roswell Park Memorial Institute (RPMI-1640) Medium (Corning®, Corning, New York), supplemented with 10% Fetal Select serum (Atlas Biologicals, Fort Collins, Colorado). The cells were grown in T-25 tissue culture flasks and incubated at 37°C, 5% CO₂. Cells were passaged every 2-3 days at 80-90% confluency.

Creation of a Stable Gene Overexpression

Antibiotic Sensitivity Curve

An antibiotic sensitivity curve assay was performed using the NCI-H1299 Cell Line to determine an optimal selection concentration of Geneticin™ selective antibiotic (G418 Sulfate – Gibco County Dublin, Ireland) to be used for selection of successful transformants. Cells were plated at 50,000 cells/well in a 12 well plate and grown overnight in RPMI-1640 medium (Corning®). Twenty-four hours post-plating; varying Geneticin™ selective antibiotic (G418 Sulfate – Gibco) concentrations were added to the wells. Concentrations ranged from 0.0 mg/mL (Control) to 1.2 mg/mL. RPMI-1640 medium was replaced every 48 hrs with cell cytopathic effects and cell death observed every 24 hrs for 14 days for the lowest concentration that killed 100% of cells.

Stable Line Generation - Transfections

One day prior to transfection, cells were plated at 50,000 cells per well in a 24 well plate in RPMI-1640 (Corning®) medium and 10% Fetal Select serum (Atlas Biologicals). The next day, NCI-H1299 cells were transfected with 0.5 ug pcDNA3.1+/-

(k)-DYK empty vector (GenScript, Piscataway, New Jersey), pcDNA3.1+/c-(k)-HPRT-DYK (GenScript) or pcDNA3.1+/c-(k)-TNFAIP8L1-DYK (GenScript) using DNA-In® transfection reagent (Molecular Transfer Inc., Gaithersburg, Maryland) according to manufacturer's instructions. The transfection process forced the cells to express TNFAIP8L1 or HPRT1 respectively, while the empty vector transfection was used as a control to verify that the plasmid itself or the transfection method was not cytotoxic to our cells. In the pcDNA3.1+/c-(k)-DYK plasmid, the DYK portion encodes for a FLAG tag which can be used to isolate the protein and protein interests of complexes through utilization of anti-FLAG antibodies. In the twenty-four hours-post-transfection, medium replaced with fresh RPMI-1640 (Corning®) medium and 10% Fetal Select serum (Atlas Biologicals). Forty-eight hours-post-transfection, cells were trypsinized with 0.25% trypsin EDTA (1x) (Gibco) and transferred to T-25 flasks. Seventy-two hours-post-transfection, RPMI-1640 medium containing 10% Fetal Select serum (Atlas Biologicals) and 0.75 mg/mL Geneticin™ selective antibiotic (G418 Sulfate-Gibco) was added to cells to select for successful transformants. Future passages of transfected cells used RPMI-1640 medium with 10% Fetal Select serum (Atlas Biologicals) and 0.75 mg/mL Geneticin™(Gibco) in order to continue selection of successful transformants.

Transient Gene Overexpression

NCI-H1299 Cells were used at 90% confluence in T-25 flasks containing RPMI-1640 (Corning®) medium and 10% Fetal Select serum (Atlas Biologicals). NCI-H1299 cells were transfected with 5.0 ug pcDNA3.1+/c-(k)-DYK empty vector (GenScript), pcDNA3.1+/c-(k)-HPRT-DYK (GenScript) or pcDNA3.1+/c-(k)-TNFAIP8L1-DYK (Genscript) using DNA-In® transfection reagent (Molecular Transfer Inc.) according to

manufacturer's instructions. All flasks were co-transfected with 1.0 ug pAdVantage™(Promega, Madison, Wisconsin), to increase protein expression of interest by increasing initiation of translation. Twenty-four hours-post-transfection, medium was replaced with new RPMI-1640(Corning®) medium and 10% Fetal Select (Atlas Biologicals). Forty-eight hours-post-transfection cells were lysed for co-immunoprecipitation.

Co-Immunoprecipitation

In order to determine putative protein interactors, TNFAIP8L1 and the interacting proteins were isolated from the cell lysate by co-immunoprecipitation. H1299 cells stably expressing TNFAIP8L1 and HPRT1 were lysed in Pierce™ IP Lysis Buffer (ThermoFisher Scientific, Waltham, Massachusetts) containing Halt™ protease and phosphatase inhibitors (ThermoFisher Scientific) for thirty mins with constant agitation at 4°C on a rotator. Following thirty-minute lysis, lysate was microcentrifuged for twenty mins at 12,000 RPM at 4°C. Supernatant was added to Anti-FLAG® M2 Magnetic Beads (Sigma-Aldrich, St. Louis, Missouri) and incubated overnight with constant agitation at 4°C on a rotator. Beads were washed with TBST (Tween-20 at 0.05%) and eluted in 2x Laemmli sample buffer (Bio-Rad, Hercules, California) containing 5% 2-mercaptoethanol (2-ME) and boiled at 100°C for three mins. Eluate was used for western blot analysis and/or mass spectrometry analysis.

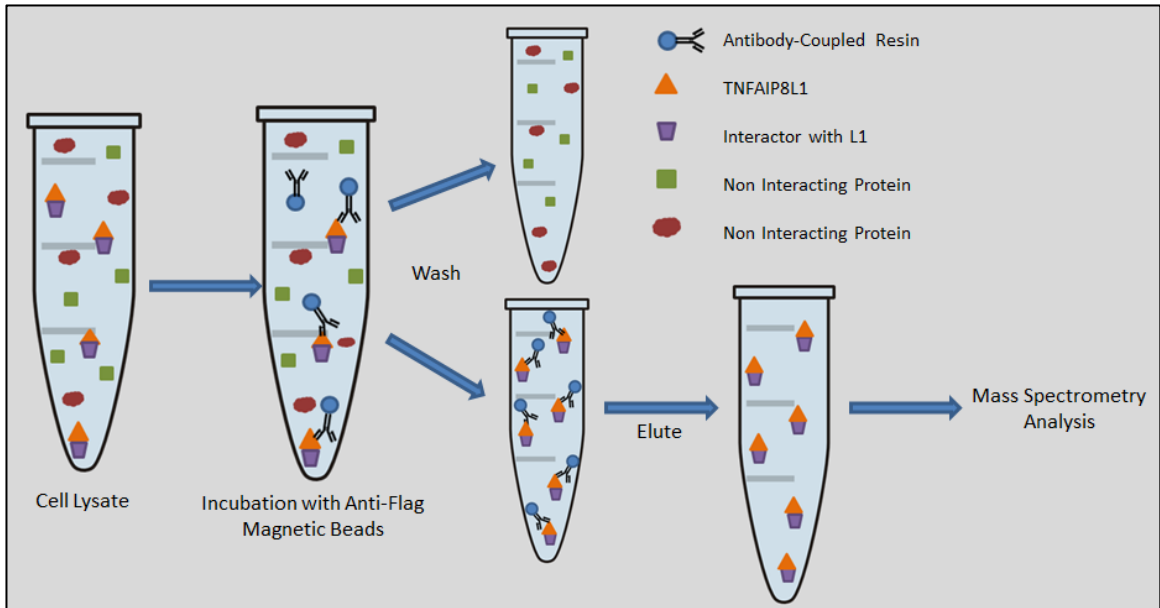


Figure 6. Co-immunoprecipitation schematic beginning with lysis of cells through incubation with Anti-FLAG[®] M2 Magnetic Beads (Sigma), wash steps and elution for western blot and mass spectrometry analysis.

Western Blots

Western blots were performed to determine that TNFAIP8L1 and HPRT1 were present in our transfected cells and therefore suitable for the next steps. Eluate in 2x loading dye with 5% 2-ME was loaded on Mini-PROTEAN[®] TGX[™] Pre-Cast gels (Bio-Rad). The PAGE gel was run in 1x Tris/Glycine/SDS Buffer (Bio-Rad) at 150 volts for 30 to 50 mins. Chameleon Duo Pre-Stained Protein Ladder was used as a standard (LI-COR Biosciences, Lincoln, Nebraska). Proteins were transferred to a nitrocellulose membrane in 1x Turbo Transfer Buffer using a Trans-Blot[®] Turbo[™] Transfer System (Bio-Rad), according to the manufacturer's protocol. REVERT[™] Total Protein stain (LI-COR) was used according to manufacturer's protocols prior to blocking blots in nonfat dried milk for visualization of potential protein interactors pulled out during co-immunoprecipitation. Blots were imaged on the Odyssey[®] CLx Infrared Imaging System (LI-COR). Membrane was then blocked in 5% non-fat dried milk in TBST (0.1% Tween

20) for 60-90 mins before incubation with rabbit DYKDDDDK tag polyclonal antibody (2 ug/mL) (Invitrogen, Carlsbad, California) overnight at 4°C on a nutator (Fisher Scientific, Hampton, New Hampshire). The nitrocellulose membrane was rinsed two times with TBST and then washed three times with TBST for 5 mins each on a rocking platform. Post washing, blot was incubated with IRDye®800CW Donkey anti-Rabbit secondary antibody (70 ng/mL) (LI-COR) for 1 hr in the dark at room temperature on a rocker. Blot was washed three times with TBST and two times with TBS before imaging on the Odyssey® CLx Infrared Imaging System (LI-COR).

Mass Spectrometry

Protein identification was achieved through Ultra-performance liquid chromatography-tandem mass spectrometry on the Q-Exactive HF-X quadrupole-Orbitrap mass spectrometer (ThermoFisher Scientific). Protein identification completed using Comet and Tandem spectral libraries. Samples were processed by Dr. Brian Balgley at Bioproximity (Chantilly, Virginia).

Sub-cloning

PCR amplifications of TNFAIP8L1, DVL3 and FBXW5 inserts were performed in 50 uL reactions with (1x) Q5® reaction buffer (New England BioLabs, Ipswich, Massachusetts), 200 nM dNTP mixture, 0.02 U/uL Q5® polymerase (New England BioLabs), 1.0 ng of template and 0.5 uM of respective primers (**Table 4**). PCR amplification of TNFAIP8L1, DVL3 and FBXW5 was run at a reaction protocol of incubation at 98°C for 30 seconds, followed by 20 cycles of 98°C for 10 seconds, 60°C for 15 seconds, 72°C for 75 seconds, and then 72°C for 5 mins and held at 12°C.

Insert	Forward Primer (BamHI)	Reverse Primer (NotI)
<i>TNFAIP8L1</i>	ACGTAT GGATCCGT ATGG ACACCTTCAG CACCAAG	ACGTAT GCGGCCGC TCAGAGGCTGCCCTCGTCCAG
<i>FBXW5</i>	ACGTAT GGATCCGT ATGGACGAGGGCGGCACGCC	ACGTAT GCGGCCGC TCAGCGCCTCTGGCTGGCAAG
<i>DVL3</i>	ACGTAT GGATCCGT ATGGGCGAGACCAAGATCAT	ACGTAT GCGGCCGC TCACATCACATCCACAAAGAA

Table 4. Forward and reverse primers used in PCR amplification of inserts *TNFAIP8L1*, *DVL3* and *FBXW5*.

Restriction digestion of PCR products was performed using BamHI and NotI to create compatible ends for ligations with pACT and pBIND vectors used in mammalian two-hybrid assays. Similarly, pACT and pBIND were subjected with restriction digestions with BamHI and NotI. Ligations were performed to generate fusion proteins with all plasmids and inserts (**Table 5**) with 50 ng vector and a 1:3 vector to insert ratio. Nuclease free water, 10x T4 ligase buffer (New England BioLabs), 50 ng vector, insert and T4 DNA ligase (New England BioLabs) were combined and ligation was run at RT for 1 hr. Ligations were then immediately used in transformations. One Shot™ Top10 competent *Escherichia coli* cells (ThermoFisher Scientific) were transformed and plated on LB-AMP (100 ug/mL) plates for selection of successful transformants. Colonies were picked and grown in LB-AMP liquid media (100ug/mL) overnight at 37°C with constant shaking. Plasmid DNA was isolated after 16 hrs using QIAprep® Spin Miniprep Kit (QIAGEN, Hilden, Germany). Glycerol stocks were made of all mini preps by adding 1 part of respective miniprep to 1 part 65% glycerol (0.1M MgSO₄, 0.025 M Tris-HCl, pH 8.0) and mixing well, then placing in -80°C.

The success of ligation was then determined for each individual transformant by separating the restriction digestion on a 1.5% agarose gel to identify correct restriction digestion pattern. The plasmids (**Table 5**) were then analyzed for correct, in-frame sequence by DNA sequencing (University of Maine Sequencing Facility) with T7 EEV primer (Promega).

Plasmids	Fusion Proteins
Positive Control: pACT-MyoD and pBIND-ID	Encodes for VP16-MyoD and GAL4-Id fusion proteins, respectively.
Negative Control: pBIND and pACT	Encode for no fusion proteins
pACT-TNFAIP8L1	Encodes for VP16-TNFAIP8L1
pACT-DVL3	Encodes for VP16-DVL3
pACT-FBXW5	Encodes for VP16-FBXW5
pBIND-TNFAIP8L1	Encodes for GAL4-TNFAIP8L1
pBIND-DVL3	Encodes for GAL4-DVL3
pBIND-FBXW5	Encodes for GAL4-FBXW5

Table 5. Summary of plasmids and fusion constructs used in mammalian two-hybrid assay.

Subcloning of Mammalian-Two Hybrid Assay Plasmids

One Shot™ Top10 competent *Escherichia coli* cells (ThermoFisher Scientific) were transformed using the pACT, pBIND and pG5luc vectors from the CheckMate™ Mammalian Two-Hybrid System (Promega) and plated out onto LB-AMP (100 ug/mL) plates for selection of successful transformants. Colonies were picked of successful transformants and grown in LB-AMP liquid medium (100 ug/mL) overnight at 37°C with constant shaking. Plasmid DNA was isolated after 16 hrs using QIAprep® Spin Miniprep Kit (QIAGEN, Hilden, Germany). Glycerol stocks were made of all minipreps by adding one part of respective miniprep to one part 65% glycerol (0.1M MgSO₄, 0.025 M Tris-HCl, pH 8.0) and mixing well, then placing stocks in -80°C.

Plasmids pcDNA3-myc3-FBXW5 (Addgene, Cambridge, Massachusetts), pDONR223-DVL3-WT (Addgene) and pcDNA3.1+/c-(k)-TNFAIP8L1-DYK (GenScript) were quadrant streaked onto LB AMP plates (100 ug/mL). Colonies were picked and grown up in LB AMP liquid medium (100 ug/mL) overnight at 37°C with constant shaking. Plasmid DNA was isolated after 16 hrs using QIAprep® Spin Miniprep Kit (QIAGEN). Glycerol stocks were made of all minipreps by adding one part of respective miniprep to one part 65% glycerol (0.1M MgSO₄, 0.025 M Tris-HCl, pH 8.0) and mixing well, then placing stocks in -80°C.

Mammalian Two-Hybrid Transfections

H1299 Cells were plated at 5,000 cells/well in a white 96 well plate and grown overnight in RPMI-1640 with 10% Fetal Select serum (Atlas Biologicals). The next day, cells were transfected using DNA-In™ (Molecular Transfer Inc.) and respective pACT and pBIND experimental plasmids (75 ng) and pG5luc (50ng) according to manufacturer's protocols (Promega) (**Table 5**). Transfected cells were placed in incubator at 37°C, 5% CO₂. Twenty-four hours later medium was replaced with fresh RPMI-1640 medium (Corning®). Forty-eight hours-post-transfection; cells were used for Dual-Luciferase® Reporter Assay (Promega).

Dual Luciferase Assay

Dual-Luciferase® Reporter Assay (Promega) Reagents were prepared according to the manufacturer's recommendations. Passive lysis buffer (PLB) was diluted to (1x) by mixing 1 volume (5x) PLB and 4 volumes distilled water. Luciferase assay reagent II (LARII) was prepared by re-suspending lyophilized luciferase assay substrate in luciferase assay buffer II. Stop & Glo reagent was prepared by adding 200 uL of (50x)

Stop & Glo Substrate to 10 mL of Stop & Glo Buffer in a glass vial. These volumes were adequate for 100 assays.

Forty-eight hours-post-transfection, RPMI-1640 medium (Corning®) with 10% Fetal Select serum (Atlas Biologicals) was removed from the H1299 cells and cells were washed with (1x) Phosphate Buffered Saline (PBS). H1299 cells were lysed with (1x) PLB for 15 mins at room temperature, on a rocker. Following lysis, cells were stored at -20°C. Forty-eight hrs later, cells were plated into a white 96 well plate for completion of the protocol. The standard Dual-Luciferase® Reporter Assay (Promega) protocol was performed according to manufacturer’s protocol using a GloMax® 96 Microplate Dual Injector Luminometer (Promega). Relative interaction values reported are ratios of firefly luciferase to *Renilla* luciferase.

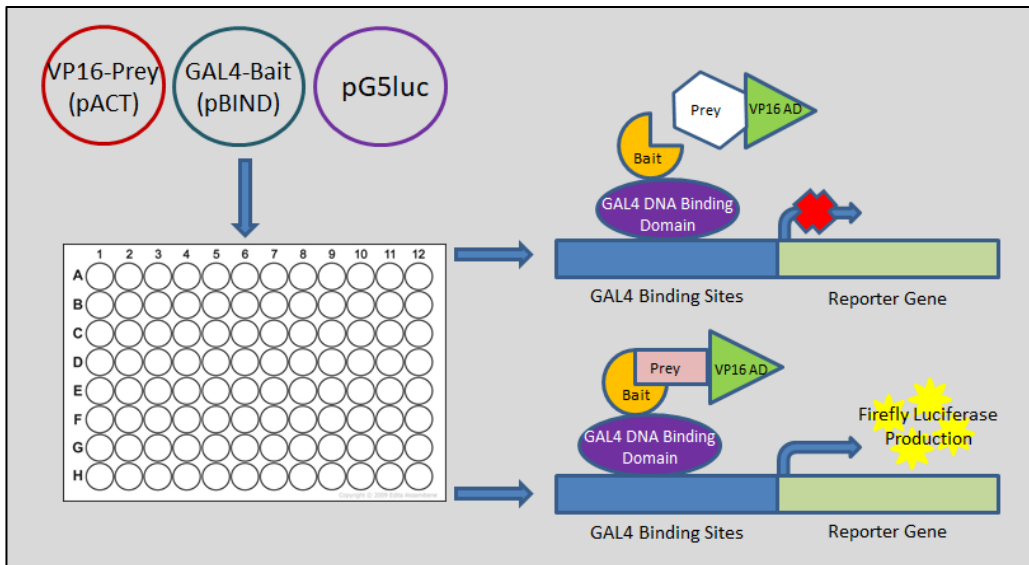


Figure 7. Schematic diagram of mammalian two-hybrid assay. Two genes of interest were cloned into the pACT and pBIND vectors to express proteins that have potential for interaction. Fusion proteins were created expressing VP16-TNFAIP8L1, GAL4-DVL3, GAL4-FBXW5 and VP16-DVL3, VP16-FBXW5, GAL4-TNFAIP8L1. The pG5luc Vector contains GAL4 binding upstream of the firefly luciferase gene. The GAL4 and VP16 fusion proteins were transfected along with the pG5luc Vector into H1299 cells. Two days post transfection; the cells were lysed and analyzed using the Dual-Luciferase® Reporter Assay System. The firefly luciferase production is relative to the protein-protein interaction occurring, however there is also *Renilla* luciferase production encoded for by the pBIND vector. This production allows for normalization of results to account for number of cells, transfection efficiency and comparison across all constructs.

RESULTS

Optimal selection concentration of Geneticin™ is 0.75 mg/mL in H1299 cells.

An antibiotic sensitivity assay was performed using the NCI-H1299 Cell Line to determine an optimal selection concentration of Geneticin™ selective antibiotic (Gibco). Cells were plated at 50,000 cells/well in a 12 well plate and grown overnight in RPMI-1640 medium (Corning®). Twenty-four hours post-plating; varying Geneticin™ selective antibiotic (G418 Sulfate – Gibco) concentrations were added to the wells. Concentrations ranged from 0.0 mg/mL (Control) to 1.2 mg/mL. RPMI-1640 (Corning®) medium was replaced every 48 hrs with cell cytopathic effects and cell death observed every 24 hrs for 14 days for the lowest concentration that killed 100% of cells. The concentration was determined to be 0.75 mg/mL.

TNFAIP8L1-FLAG Overexpressed in H1299 cells.

An antibiotic sensitivity assay was performed using the NCI-H1299 Cell Line to determine an optimal selection concentration of Geneticin™ selective antibiotic to be 0.75 mg/mL. H1299 cells were transfected with pcDNA3.1+/c-(k)-DYK empty vector (GenScript), pcDNA3.1+/c-(k)-HPRT-DYK (GenScript) or pcDNA3.1+/c-(k)-TNFAIP8L1-DYK. Verification of successful stable TNFAIP8L1 overexpression in H1299 lung cancer cell line was completed through western blot analysis. Results indicate that the TNFAIP8L1 transfection was successful with the presence of a band around 18 kDa. The empty-FLAG negative control showed a band that was unexpected, around 12.5 kDa. The HPRT1-FLAG positive control for non-specific binding was visualized as a band around 19 kDa (**Figure 8**). The bands were seen at lower molecular

are seen separately due to the presence of 2-mercaptoethanol breaking the antibody chains apart.

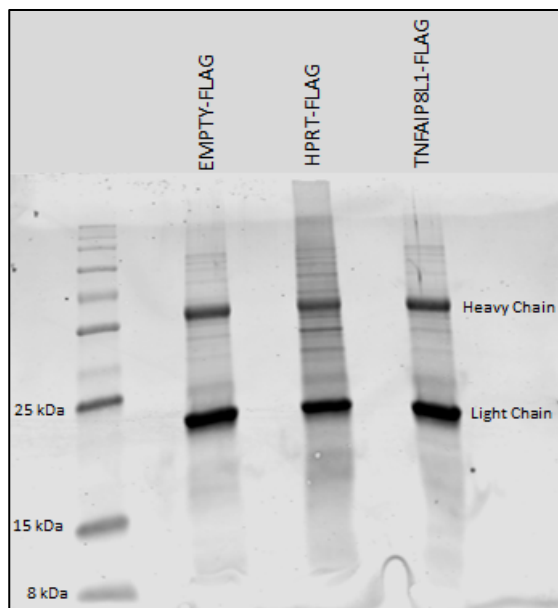


Figure 9. REVERT™ Total Protein Stain was used prior to blocking blots in non-fat dried milk for visualization of protein interactors pulled out during co-immunoprecipitation. Blot imaged on Odyssey® CLx Infrared Imaging System (LI-COR). Bands indicate total protein. TNFAIP8L1-FLAG in lane 3 shows proteins pulled out with TNFAIP8L1 during co-immunoprecipitation.

TNFAIP8L1 has 138 putative protein interactors in H1299 lung cancer cell line model.

Identification of putative protein interactors with TNFAIP8L1 was performed utilizing co-immunoprecipitation and mass spectrometry. Co-immunoprecipitation was performed using Anti-FLAG® M2 Magnetic Beads. Beads were frozen and subsequently eluted with FLAG peptide. Eluate was analyzed using Ultra-performance liquid chromatography-tandem mass spectrometry on the Q-Exactive HF-X quadrupole-Orbitrap mass spectrometer (ThermoFisher) by Bioproximity. Protein identification was completed using Comet and Tandem spectral libraries. There were 561 unique genes encoding proteins that were interacting with our negative control (empty) and 181 unique

genes encoding proteins that were interacting with our HPRT1 control for non-specific binding. There were 31 genes encoding proteins that were interacting with both TNFAIP8L1 and HPRT1, and 92 genes encoding proteins that were interacting with all three. There were 138 unique genes identified that encode for proteins interacting solely with TNFAIP8L1 (**Figure 10, Table 6, Supplementary Table 1**). The genes play various roles in biological processes according to gene ontology analysis with the PANTHER classification system. Of the 138 genes, 27% encode proteins involved in cellular processes including cell recognition and cell cycle regulation (**Figure 11**). A web of genes was analyzed to show protein interactions using NetworkAnalyst to visualize interactors as they relate to specific processes and each other (**Figure 12a**). Interactors involved in cell cycle regulation are shown in blue (**Figure 12a**) and pulled out for better visualization (**Figure 12b**). The genes are shown in their biological networks to narrow in on their relationships and commonalities in functions.

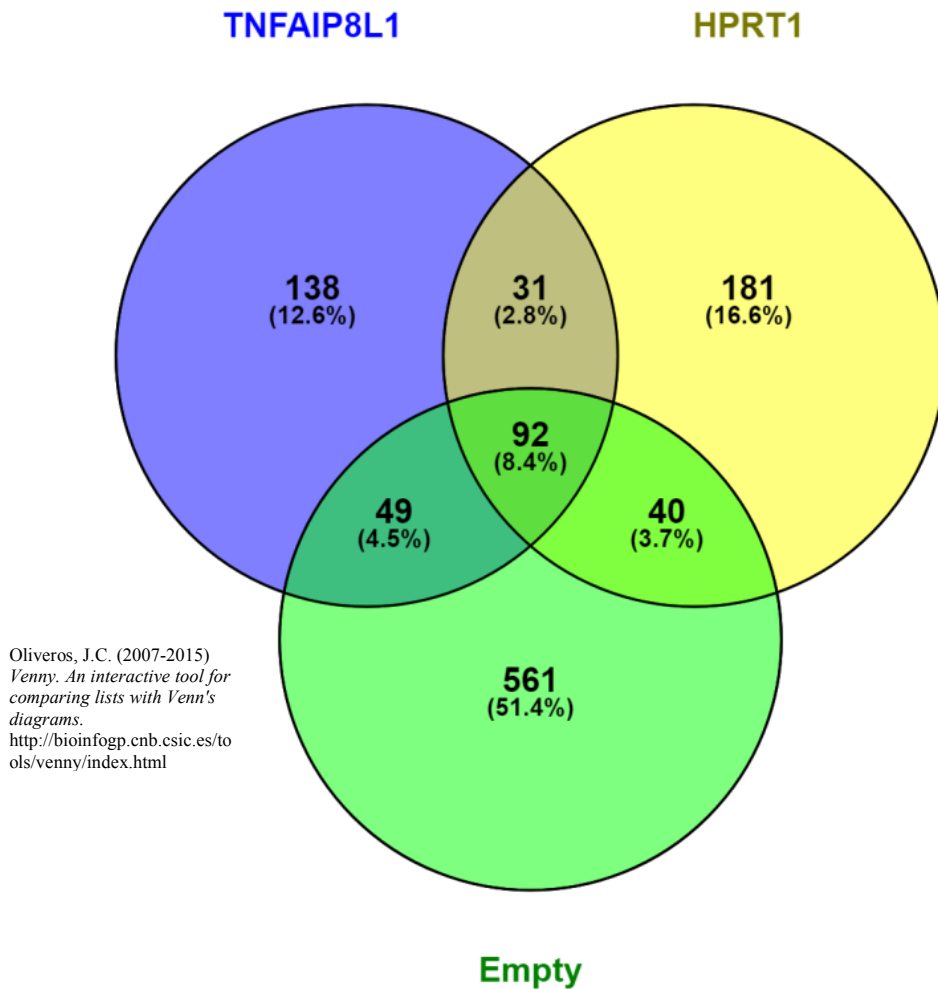


Figure 10. Venn diagram representing number of genes that encode for proteins interacting with the proteins of interest. Green represents the empty-FLAG H1299 cells, yellow represent HPRT1-FLAG and purple represents the TNFAIP8L1. There are 561,181 and 138 unique genes respectively.

Unique Interactors with TNFAIP8L1					
ENSG00000007174	ENSG00000116544	ENSG00000140264	ENSG00000164032	ENSG00000180573	ENSG00000203812
ENSG00000007933	ENSG00000120051	ENSG00000140326	ENSG00000164309	ENSG00000180938	ENSG00000205336
ENSG000000053371	ENSG00000120251	ENSG00000140836	ENSG00000164506	ENSG00000181218	ENSG00000241127
ENSG000000055044	ENSG00000122126	ENSG00000141068	ENSG00000164508	ENSG00000181752	ENSG00000246705
ENSG000000055609	ENSG00000123219	ENSG00000142544	ENSG00000165078	ENSG00000183019	ENSG00000258839
ENSG000000064787	ENSG00000125675	ENSG00000142784	ENSG00000167210	ENSG00000184260	ENSG00000260220
ENSG000000066248	ENSG00000126001	ENSG00000143344	ENSG00000167332	ENSG00000185238	ENSG00000267680
ENSG000000070367	ENSG00000126016	ENSG00000143952	ENSG00000167716	ENSG00000187166	ENSG00000270467
ENSG000000073734	ENSG00000127507	ENSG00000144455	ENSG00000168264	ENSG00000187950	ENSG00000270505
ENSG000000074071	ENSG00000128512	ENSG00000147381	ENSG00000168906	ENSG00000188171	ENSG00000272196
ENSG000000080345	ENSG00000128881	ENSG00000148200	ENSG00000169594	ENSG00000188486	ENSG00000274997
ENSG000000088387	ENSG00000130177	ENSG00000149503	ENSG00000170364	ENSG00000188487	ENSG00000275221
ENSG00000100014	ENSG00000132746	ENSG00000152578	ENSG00000170485	ENSG00000196159	ENSG00000276021
ENSG00000100804	ENSG00000133067	ENSG00000154252	ENSG00000171843	ENSG00000196218	ENSG00000276126
ENSG00000105968	ENSG00000135406	ENSG00000155511	ENSG00000172464	ENSG00000196547	ENSG00000276289
ENSG00000107863	ENSG00000135480	ENSG00000156136	ENSG00000174137	ENSG00000196646	ENSG00000276368
ENSG00000108469	ENSG00000135517	ENSG00000156787	ENSG00000175221	ENSG00000196747	ENSG00000276903
ENSG00000109189	ENSG00000136250	ENSG00000159433	ENSG00000175573	ENSG00000196787	ENSG00000277075
ENSG00000110811	ENSG00000137522	ENSG00000160094	ENSG00000176624	ENSG00000196866	ENSG00000277603
ENSG00000113327	ENSG00000137872	ENSG00000163110	ENSG00000176946	ENSG00000197535	ENSG00000278463
ENSG00000113719	ENSG00000138600	ENSG00000163214	ENSG00000177030	ENSG00000197705	ENSG00000278677
ENSG00000115705	ENSG00000138767	ENSG00000163904	ENSG00000177398	ENSG00000198863	ENSG00000281179
ENSG00000116120	ENSG00000139990	ENSG00000163913	ENSG00000179869	ENSG00000203710	ENSG00000282988

Table 6. A comprehensive list of all 138 genes that encode for protein interactors with TNFAIP8L1 arranged by their ENSEMBL nomenclature.

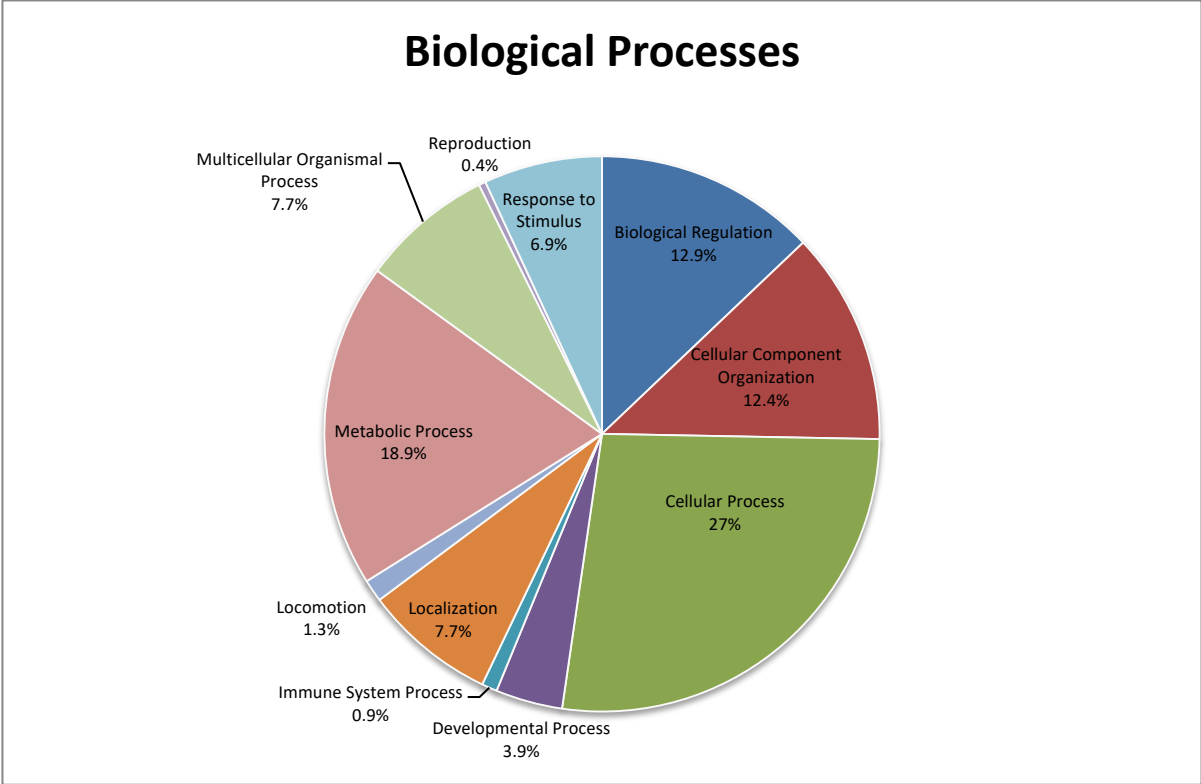
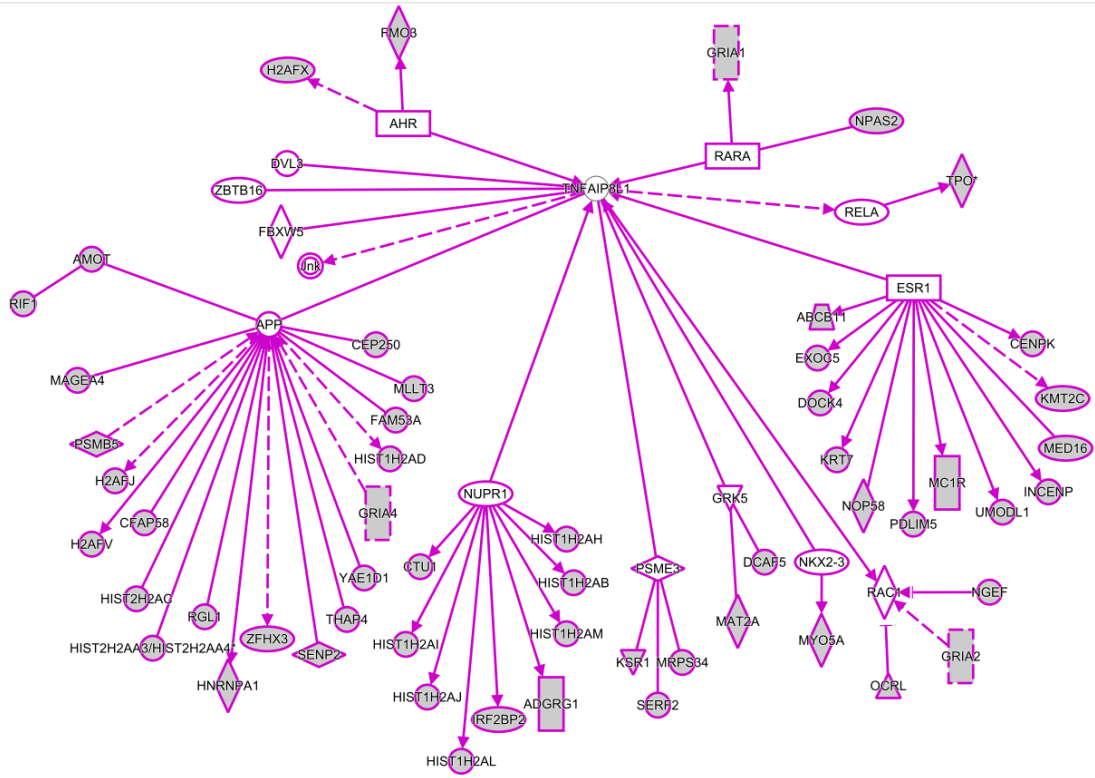
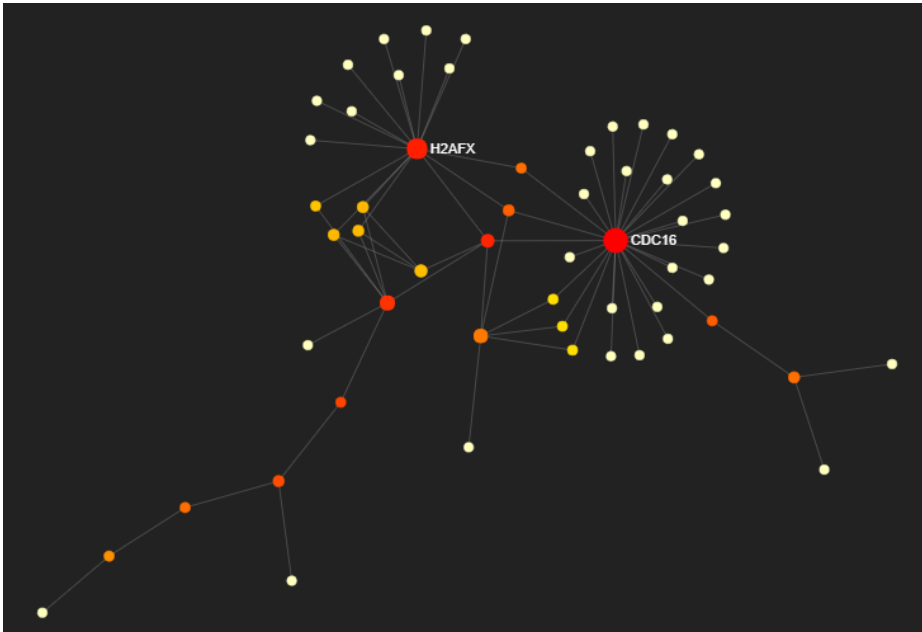


Figure 11. Summary of 138 genes for unique protein interactors with TNFAIP8L1 as they relate to biological processes using the PANTHER classification system for analysis.

A**B**

C

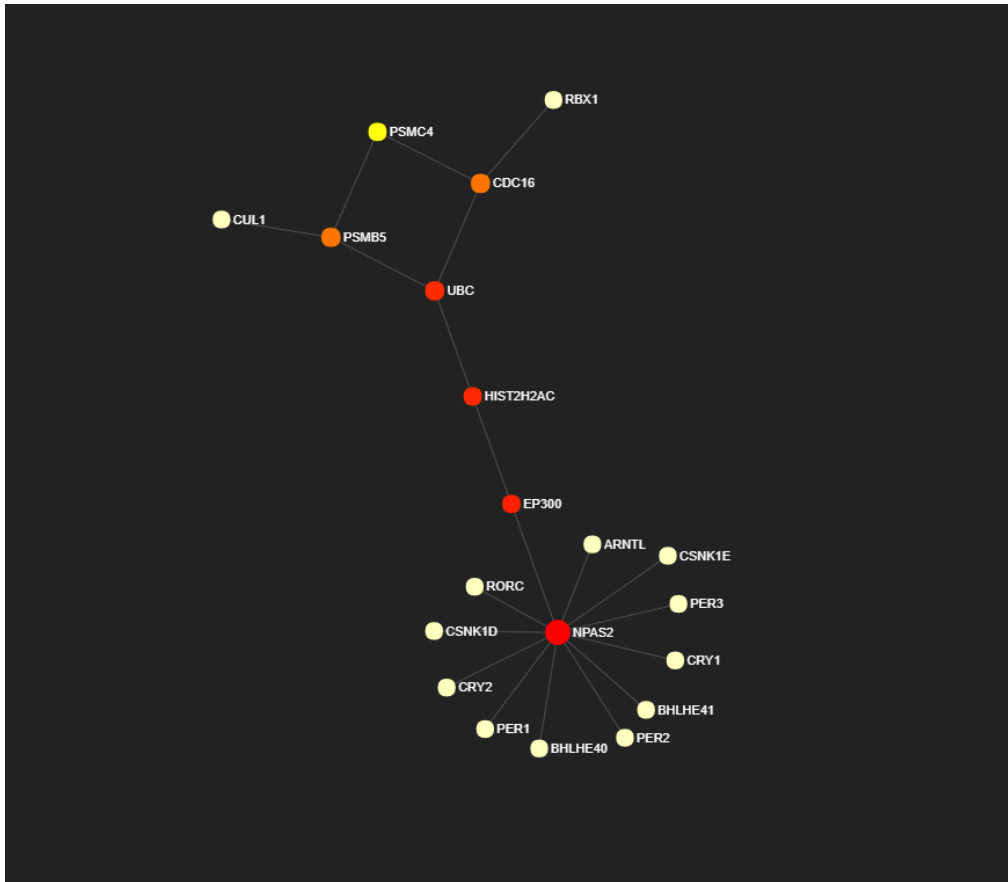


Figure 12 (A) Network that relates genes and proteins with known TNFAIP8L1 interactions to putative protein interactions from mass spectrometry data using Ingenuity Pathways software. Dotted lines represent indirect interactions and solid lines represent direct interactions. White shapes are presumably primary interactors and grey shapes, secondary interactors. Network Shapes defined in key to the right of the figure. (B) Cell Cycle interactors singled out from other interactors (Xia 2015, 2018). (C) Circadian rhythm interactors singled out from other interactors (Xia 2015, 2018).

TNFAIP8L1 does not interact directly with DVL3 or FBXW5.

Validation of expected protein-protein interactions with TNFAIP8L1 from research previously published (Chatr-Aryamontri et al., 2017; Ha et al., 2014) was not verified through mammalian two-hybrid assay. Relative interaction was calculated as a ratio of firefly luciferase activity to *Renilla* luciferase activity and reported as individual points representing replicates (**Figure 13, Supplementary Figure 1**). *Renilla* luciferase activity is encoded for in the pBIND vector allowing stable activity of *Renilla* to be used

as an internal control. This activity is independent of interactions and allows for normalization between samples with different cell numbers and transfection efficiencies. Controls were performed with 4 replicates each and experimental wells had 8 replicates for each. TNFAIP8L1 was expected to interact with DVL3 and FBXW5, but our results did not support evidence of an interaction. FBXW5 was validated as an interactor with TNFAIP8L1 (Ha et al., 2014) and DVL3 was previously determined to be a potential interactor, but not validated (Rual et al., 2005).

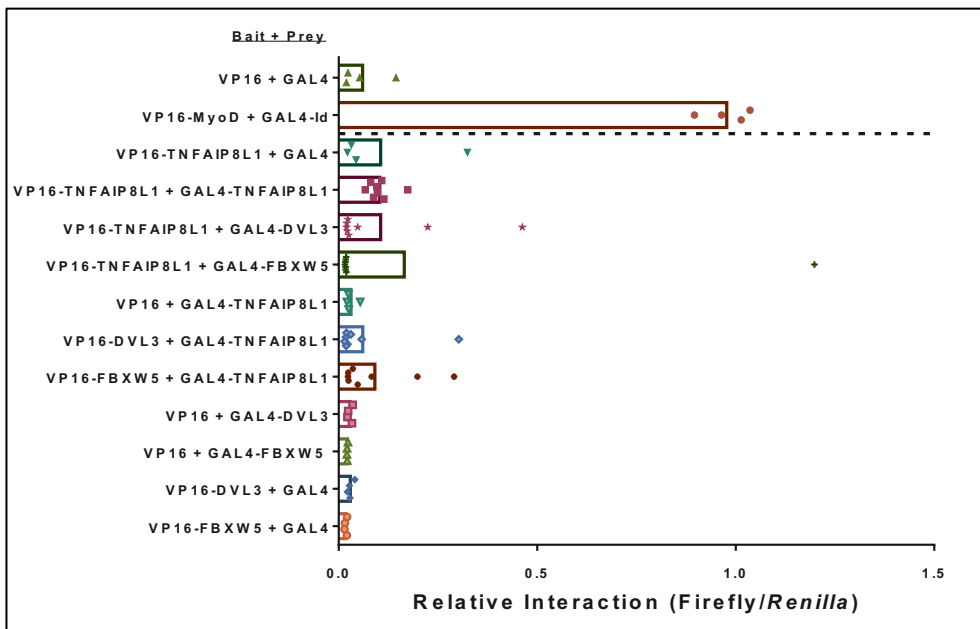


Figure 13. Results of mammalian two-hybrid assay. The fusion construct VP16-MyoD + GAL4-Id was used as a positive control. Relative interaction was calculated as a ratio of firefly luciferase activity to *Renilla* luciferase activity. Individual points represent replicates. Controls were performed with 4 replicates each and experimental wells had 8 replicates for each. No significant interaction between experimental constructs was seen in either experiment.

DISCUSSION

With cancer near the top of the most prevalent diseases list for diagnoses and fatalities and poised to stay there, it is critical to understand the processes that govern it. An expanded understanding of tumorigenesis pathways and proteins that act in these pathways can guide us to new prevention tactics as well as to better aimed treatment options, which are highly sought after today. Previous studies of TNFAIP8L1 since its discovery in 2008 have left it relatively uncharacterized, and surrounded by many questions about its role in tumorigenesis and immunity. The putative protein interactors identified in this study provide a place to start when looking at its role and functions as a tumor suppressor.

There were 138 putative protein interactors with TNFAIP8L1 identified in this study (**Table 6, Supplementary Table 1**). A gene ontology study using the PANTHER (Protein ANalysis THrough Evolutionary Relationships) classification system revealed that there was a wide variety of biological processes implicated by interactors. The majority encoded for proteins involved in cellular processes (27%), followed by metabolic processes (18.9%), biological regulation (12.9%), cellular component organization (12.4%), multicellular organismal processes (7.7%), localization (7.7%), response to stimulus (6.9%), developmental processes (3.9%), locomotion (1.3%), immune system processes (0.9%) and reproduction (0.4%) (**Figure 11**). The cellular processes portion was further broken down into cell communication (54.3%), cellular component movement (20%), cell cycle regulation (11.4%), cell growth (5.7%), cell recognition (5.7%), and cytokinesis (2.9%). The data suggest the TNFAIP8L1 plays a

role in many different biological processes and pathways particularly those involving cellular processes such as cell communication and the cell cycle (**Figure 12b**). It is also interesting to note that only 0.9% of genes encoding proteins that interacted with TNFAIP8L1 control immune system processes, as it is believed that the *TNFAIP8* gene family plays a role in immunity.

There were several genes of interest that were pulled out including melanoma-associated antigen 4 (*MAGEA4*) and angiomin (AMOT) (**Figure 12a**). *MAGEA4* encodes for the following proteins C9JK50, C9JIR1, Q1RN33, C9JZJ5, P43358, Q4V9T5, C9J9C2 pulled out in the mass spectrometry analysis of interactors. The *MAGE-A* gene family is expressed in numerous solid tumors, but silent in normal tissues except for male germline cells, which do not carry human leukocyte antigen (HLA) molecules. The proteins encoded for by the *MAGE-A* family are recognized by cytotoxic T-lymphocytes and allow for an immune response against tumor tissue (Hamosh, Scott, Amberger, Valle, & McKusick, 2000). In a study from 2000, 28% of patients with Hodgkin's lymphoma expressed *MAGEA4* indicating that *MAGEA4* may be involved in Hodgkin's lymphoma and a target for immunotherapy (Chambost et al., 2000).

Angiomin (AMOT) is believed to play a role in the formation of new blood vessels, a process termed angiogenesis, and its regulation. Angiogenesis is necessary for tumors to grow and is therefore a topic of interest in tumorigenesis studies. AMOT has also been implicated in WNT signaling pathways, which is key for regulating development and previously associated with cancer (Z. Li et al., 2012). The WNT pathway is involved in signaling to the disheveled protein family, which includes DVL3. This link between TNFAIP8L1, AMOT, the WNT pathway and DVL3 could be

significant in understanding the underlying mechanisms of tumorigenesis and how TNFAIP8L1 plays a role.

Another interactor of interest was Neuronal PAS Domain Protein 2 (NPAS2), as it is associated circadian rhythm pathways (**Figure 12c**) and related genes (DeBruyne, Weaver, & Reppert, 2007; Landgraf, Wang, Diemer, & Welsh, 2016). The circadian clock is an internal time keeping system that regulates physiological processes and ultimately rhythms in gene expression that alter metabolism and behavior. Circadian rhythms regulate processes that alter physical, mental and behavioral changes. The rhythms can be disrupted and disruptions are linked to an increased risk of cancer development. In 2001, the Fred Hutchinson Cancer Research center showed nurses who regularly work the night shift were more likely to be diagnosed with cancer (Engel, 2014) and 10 years ago the International Agency for research on cancer classified night shift work as carcinogenic. While there is link between circadian disruption and cancer, as well as TNFAIP8L1 and circadian rhythm pathways, the mechanism of the links are unknown. TNFAIP8L1 may be playing a role in this pathway and its regulation in tumorigenesis.

These putative protein interactions, once validated, will lead to increased understanding of protein interaction pathways regulating the mechanism of tumorigenesis and ultimately the TNFAIP8L1 binding partners may serve as potential partners for future drug therapy and cancer prevention/treatment options.

The mammalian two-hybrid validations in this experiment did not support our hypothesis or previous data suggesting FBXW5 and DVL3 interact directly with TNFAIP8L1. Issues validating interactors may be because they are not directly binding

TNFAIP8L1, but are part of a larger complex of proteins, or it is also possible that our system does not allow for post translational modifications to occur that are required for binding. Conversely, there could be post translational modifications occurring that are not true to biological function.

In the future validation of putative TNFAIP8L1 protein interactors could be performed using mammalian two-hybrid assays, but considerations of the systems shortcomings should be considered. A proximity ligation assay or other means of visualizing interactions such as bimolecular fluorescence complementation may be necessary. Performing a similar protein interaction study with TNFAIP8, TNFAIP8L2, and TNFAIP8L3 would be beneficial in increasing our understanding of the gene family, but also elucidate possible pathways to study for the individual members. Validated interactions should lead into mutagenesis studies to identify specific binding domains of TNFAIP8L1 and its binding partner as a way to identify possible clinical benefits. Previous studies have shown that TNFAIP8L1 plays a role in tumorigenesis and this current study asking what pathways it was involved with and through which protein interactions has revealed a large list of interactors to be validated and further studied. The importance of elucidating the function of TNFAIP8L1 lies in its importance as a tumor suppressor, as it could lead to new avenues of study and eventually target specific treatments for cancer.

REFERENCES

- American Cancer Society. (2016). Summary of the ACS Guidelines on Nutrition and Physical Activity. Retrieved from <https://www.cancer.org/healthy/eat-healthy-get-active/acs-guidelines-nutrition-physical-activity-cancer-prevention/summary.html>
- American Cancer Society. (2018a). Economic Impact of Cancer. Retrieved from <https://www.cancer.org/cancer/cancer-basics/economic-impact-of-cancer.html>
- American Cancer Society. (2018b). Key Statistics for Small Cell Lung Cancer. Retrieved from <https://www.cancer.org/cancer/small-cell-lung-cancer/about/key-statistics.html>
- American Type Culture Collection. (2016). NCI-H1299 (ATCC® CRL-5803™). Retrieved from <https://www.atcc.org/en/Products/All/CRL-5803.aspx>
- Breci, L. (2017). Mass Spec - Chemistry LibreTexts. Retrieved from https://chem.libretexts.org/Core/Analytical_Chemistry/Instrumental_Analysis/Mass_Spectrometry/Mass_Spec
- Cancer Statistics - National Cancer Institute. (2017). Retrieved from <https://www.cancer.gov/about-cancer/understanding/statistics>
- Cao, X., Zhang, L., Shi, Y., Sun, Y., Dai, S., Guo, C., ... Zhang, L. (2013). Human tumor necrosis factor (TNF)-alpha-induced protein 8-like 2 suppresses hepatocellular carcinoma metastasis through inhibiting Rac1. *Molecular Cancer*, 12(1). <https://doi.org/10.1186/1476-4598-12-149>
- Cell Culture Basics Handbook*. (2016). ThermoFisher Scientific. Retrieved from <https://www.thermofisher.com/content/dam/LifeTech/global/life-sciences/CellCultureandTransfection/pdfs/Gibco-Cell-Culture-Basics-Handbook-Global.pdf>
- Center for Disease Control and Prevention. (2017). What Are the Risk Factors for Lung Cancer? Retrieved from https://www.cdc.gov/cancer/lung/basic_info/risk_factors.htm
- Center for Disease Control and Prevention. (2018). How to Prevent Cancer or Find It Early. Retrieved from <https://www.cdc.gov/cancer/dcpc/prevention/index.htm>
- Chambost, H., Van Baren, N., Brasseur, F., Godelaine, D., Xerri, L., Landi, S. J., ... Olive, D. (2000). Expression of gene MAGE-A4 in Reed-Sternberg cells. *Blood*, 95(11), 3530–3533. Retrieved from <http://www.bloodjournal.org/content/95/11/3530.abstract>
- Chatr-Aryamontri, A., Oughtred, R., Boucher, L., Rust, J., Chang, C., Kolas, N. K., ... Tyers, M. (2017). The BioGRID interaction database: 2017 update. *Nucleic Acids Research*, 45(D1), D369–D379. <https://doi.org/10.1093/nar/gkw1102>
- Chen, L., Yang, X., Yang, X., Fan, K., Xiao, P., Zhang, J., & Wang, X. (2016). Association between the expression levels of tumor necrosis factor- α -induced protein 8 and the prognosis of patients with gastric adenocarcinoma. *Experimental and Therapeutic Medicine*, 12(1), 238–244. <https://doi.org/10.3892/etm.2016.3327>

- Cheng, Y., Yu, P., Duan, X., Liu, C., Xu, S., Chen, Y., ... Tao, Z. (2015). Genome-wide analysis of androgen receptor binding sites in prostate cancer cells. *Experimental and Therapeutic Medicine*, 9(6), 2319–2324. <https://doi.org/10.3892/etm.2015.2406>
- Cottrell, J. S. (2011). Protein identification using MS/MS data. *Journal of Proteomics*. <https://doi.org/10.1016/j.jprot.2011.05.014>
- Cui, J., Hao, C., Zhang, W., Shao, J., Zhang, N., Zhang, G., & Liu, S. (2015). Identical Expression Profiling of Human and Murine TIPE3 Protein Reveals Links to Its Functions. *Journal of Histochemistry and Cytochemistry*, 63(3), 206–216. <https://doi.org/10.1369/0022155414564871>
- Cui, J., Zhang, G., Hao, C., Wang, Y., Lou, Y., Zhang, W., ... Liu, S. (2011). The expression of TIPE1 in murine tissues and human cell lines. *Molecular Immunology*, 48(12–13), 1548–1555. <https://doi.org/10.1016/j.molimm.2011.04.023>
- Dammeyer, T., & Schobert, M. (2010). Interactomics. In *Handbook of Hydrocarbon and Lipid Microbiology* (pp. 4407–4428). Berlin, Heidelberg: Springer Berlin Heidelberg. https://doi.org/10.1007/978-3-540-77587-4_345
- DeBruyne, J. P., Weaver, D. R., & Reppert, S. M. (2007). CLOCK and NPAS2 have overlapping roles in the suprachiasmatic circadian clock. *Nature Neuroscience*, 10(5), 543–545. <https://doi.org/10.1038/nn1884>
- Deng, B., Feng, Y., & Deng, B. (2015). TIPE2 Mediates the Suppressive Effects of Shikonin on MMP13 in Osteosarcoma Cells. *Cellular Physiology and Biochemistry: International Journal of Experimental Cellular Physiology, Biochemistry, and Pharmacology*, 37(6), 2434–2443. <https://doi.org/10.1159/000438596>
- Edmondson, R., Broglie, J. J., Adcock, A. F., & Yang, L. (2014). Three-Dimensional Cell Culture Systems and Their Applications in Drug Discovery and Cell-Based Biosensors. *ASSAY and Drug Development Technologies*, 12(4), 207–218. <https://doi.org/10.1089/adt.2014.573>
- Eisele, L., Klein-Hitpass, L., Chatzimanolis, N., Opalka, B., Boes, T., Seeber, S., ... Flashshove, M. (2007). Differential expression of drug-resistance-related genes between sensitive and resistant blasts in acute myeloid leukemia. *Acta Haematologica*, 117(1), 8–15. <https://doi.org/10.1159/000096854>
- Engel, M. (2014). How the circadian clock may affect cancer. Retrieved from <https://www.fredhutch.org/en/news/center-news/2014/05/Cancer-and-circadian-clock.html>
- Fang, F. C., & Casadevall, A. (2011). Reductionistic and holistic science. *Infection and Immunity*, 79(4), 1401–1404. <https://doi.org/10.1128/IAI.01343-10>
- Fayngerts, S. A., Wu, J., Oxley, C. L., Liu, X., Vourekas, A., Cathopoulos, T., ... Chen, Y. H. (2014a). TIPE3 is the transfer protein of lipid second messengers that promote cancer. *Cancer Cell*, 26(4), 465–478. <https://doi.org/10.1016/j.ccr.2014.07.025>
- Fayngerts, S. A., Wu, J., Oxley, C. L., Liu, X., Vourekas, A., Cathopoulos, T., ... Chen, Y. H. (2014b). TIPE3 is the transfer protein of lipid second messengers that promote cancer. *Cancer Cell*, 26(4), 465–478. <https://doi.org/10.1016/j.ccr.2014.07.025>

- Free, R. B., Hazelwood, L. A., & Sibley, D. R. (2009). Identifying novel protein-protein interactions using co-immunoprecipitation and mass spectroscopy. *Current Protocols in Neuroscience*. <https://doi.org/10.1002/0471142301.ns0528s46>
- Giovanella, B. C., Yim, S. O., Stehlin, J. S., & Williams, L. J. (1972). Development of invasive tumors in the “nude” mouse after injection of cultured human melanoma cells. *Journal of the National Cancer Institute*, *48*(5), 1531–1533. Retrieved from <http://www.ncbi.nlm.nih.gov/pubmed/5030962>
- Ha, J. Y., Kim, J. S., Kang, Y. H., Bok, E., Kim, Y. S., & Son, J. H. (2014). Tnfaip8^{fl/Oxi-??} binds to FBXW5, increasing autophagy through activation of TSC2 in a Parkinson’s disease model. *Journal of Neurochemistry*, *129*(3), 527–538. <https://doi.org/10.1111/jnc.12643>
- Hamosh, A., Scott, A. F., Amberger, J., Valle, D., & McKusick, V. A. (2000). Online Mendelian Inheritance in Man (OMIM). *Human Mutation*, *15*(1), 57–61. [https://doi.org/10.1002/\(SICI\)1098-1004\(200001\)15:1<57::AID-HUMU12>3.0.CO;2-G](https://doi.org/10.1002/(SICI)1098-1004(200001)15:1<57::AID-HUMU12>3.0.CO;2-G)
- Hanahan, D., & Weinberg, R. A. (2000). The hallmarks of cancer. *Cell*, *100*(1), 57–70. <https://doi.org/10.1007/s00262-010-0968-0>
- Hanahan, D., & Weinberg, R. A. (2011). Hallmarks of cancer: The next generation. *Cell*. <https://doi.org/10.1016/j.cell.2011.02.013>
- Harvard School of Public Health. (2015). WHO report says eating processed meat is carcinogenic: Understanding the findings. Retrieved from <https://www.hsph.harvard.edu/nutritionsource/2015/11/03/report-says-eating-processed-meat-is-carcinogenic-understanding-the-findings/>
- Kumar, D., Gokhale, P., Broustas, C., Chakravarty, D., Ahmad, I., & Kasid, U. (2004). Expression of SCC-S2, an antiapoptotic molecule, correlates with enhanced proliferation and tumorigenicity of MDA-MB 435 cells. *Oncogene*, *23*(2), 612–616. <https://doi.org/10.1038/sj.onc.1207123>
- Landgraf, D., Wang, L. L., Diemer, T., & Welsh, D. K. (2016). NPAS2 Compensates for Loss of CLOCK in Peripheral Circadian Oscillators. *PLoS Genetics*, *12*(2). <https://doi.org/10.1371/journal.pgen.1005882>
- Li, Y., Li, X., Liu, G., Sun, R., Wang, L., Wang, J., & Wang, H. (2015). Downregulated TIPE2 is associated with poor prognosis and promotes cell proliferation in non-small cell lung cancer. *Biochemical and Biophysical Research Communications*, *457*(1), 43–49. <https://doi.org/10.1016/j.bbrc.2014.12.080>
- Li, Z., Wang, Y., Zhang, M., Xu, P., Huang, H., Wu, D., & Meng, A. (2012). The Amotl2 Gene Inhibits Wnt/ β -Catenin Signaling and Regulates Embryonic Development in Zebrafish. *The Journal of Biological Chemistry*, *287*(16), 13005–13015. <https://doi.org/10.1074/jbc.M112.347419>
- Liu, K., Qin, C.-K., Wang, Z.-Y., Liu, S.-X., Cui, X.-P., & Zhang, D.-Y. (2012). Expression of tumor necrosis factor-alpha-induced protein 8 in pancreas tissues and its correlation with epithelial growth factor receptor levels. *Asian Pacific Journal of Cancer Prevention : APJCP*, *13*(3), 847–850. Retrieved from

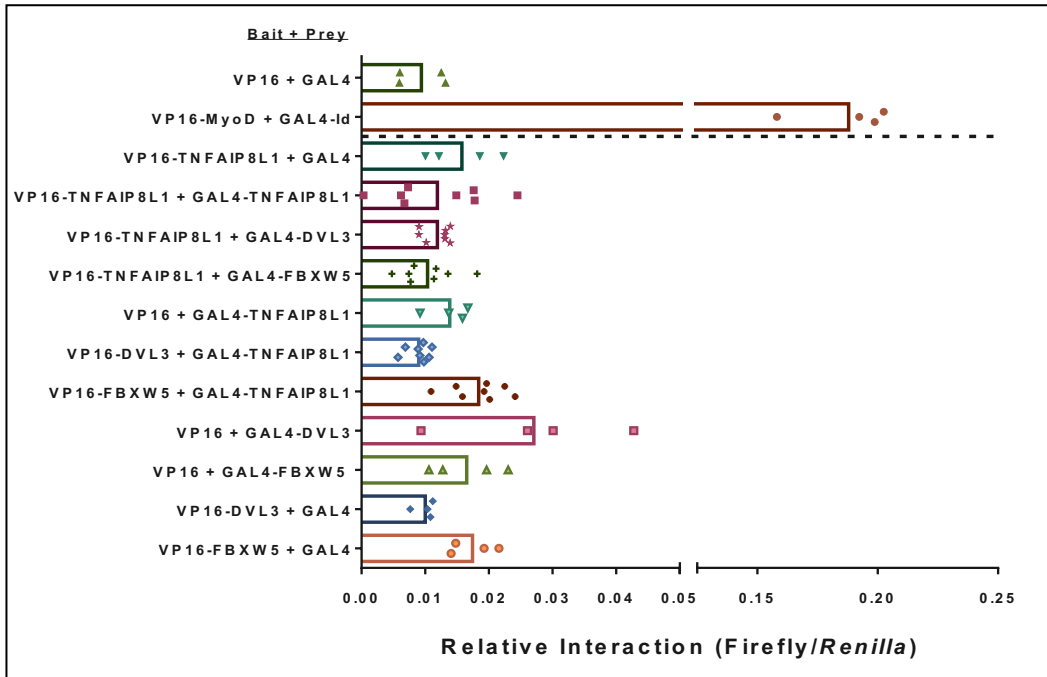
- <http://www.ncbi.nlm.nih.gov/pubmed/22631659>
- Lou, Y., & Liu, S. (2011). The TIPE (TNFAIP8) family in inflammation, immunity, and cancer. *Molecular Immunology*. <https://doi.org/10.1016/j.molimm.2011.08.006>
- Lowe, J. M., Nguyen, T. A., Grimm, S. A., Gabor, K. A., Peddada, S. D., Li, L., ... Fessler, M. B. (2017). The novel p53 target TNFAIP8 variant 2 is increased in cancer and offsets p53-dependent tumor suppression. *Cell Death and Differentiation*, *24*(1), 181–191. <https://doi.org/10.1038/cdd.2016.130>
- Mollica, M., Nemeth, L., Newman, S. D., & Mueller, M. (2015). Quality of Life in African American Breast Cancer Survivors An Integrative Literature Review. *CANCER NURSING*, *38*(3), 194–204. <https://doi.org/10.1097/NCC.0000000000000160>
- Moresco, J. J., Carvalho, P. C., & Yates, J. R. (2010). Identifying components of protein complexes in *C. elegans* using co-immunoprecipitation and mass spectrometry. *Journal of Proteomics*. <https://doi.org/10.1016/j.jprot.2010.05.008>
- National Cancer Institute. (2015). What is Cancer? Retrieved from <https://www.cancer.gov/about-cancer/understanding/what-is-cancer>
- National Cancer Institute. (2017). Types of Cancer Treatment. Retrieved from <https://www.cancer.gov/about-cancer/treatment/types>
- National Institute of Health. (2013). RePORT Cancer. Retrieved from <https://report.nih.gov/nihfactsheets/ViewFactSheet.aspx?csid=75>
- Peng, Y., Zhao, Q., Zhang, H., Han, B., Liu, S., Han, M., & Liu, S. (2016). TIPE2, a negative regulator of TLR signaling, regulates p27 through IRF4-induced signaling. *Oncology Reports*, *35*(4), 2480–2486. <https://doi.org/10.3892/or.2016.4562>
- Personalized Medicine. (n.d.). Retrieved from <http://mayoresearch.mayo.edu/center-for-individualized-medicine/personalized-medicine.asp>
- Porturas, T. P., Sun, H., Buchlis, G., Lou, Y., Liang, X., Cathopoulos, T., ... Chen, Y. H. (2015). Crucial Roles of TNFAIP8 Protein in Regulating Apoptosis and Listeria Infection. *The Journal of Immunology*, *194*(12), 5743–5750. <https://doi.org/10.4049/jimmunol.1401987>
- Rual, J.-F., Venkatesan, K., Hao, T., Hirozane-Kishikawa, T., Dricot, A., Li, N., ... Vidal, M. (2005). Towards a proteome-scale map of the human protein–protein interaction network. *Nature*, *437*(7062), 1173–1178. <https://doi.org/10.1038/nature04209>
- Siegel, R. L., Miller, K. D., & Jemal, A. (2017). Cancer statistics, 2017. *CA: A Cancer Journal for Clinicians*, *67*(1), 7–30. <https://doi.org/10.3322/caac.21387>
- Sullivan, C., Lage, C. R., Yoder, J. A., Postlethwait, J. H., & Kim, C. H. (2017). Evolutionary divergence of the vertebrate TNFAIP8 gene family: Applying the spotted gar orthology bridge to understand ohnolog loss in teleosts. *PLoS ONE*, *12*(6). <https://doi.org/10.1371/journal.pone.0179517>
- Wang, Q. J., Knezetic, J. A., Schally, A. V., Pour, P. M., & Adrian, T. E. (1996). Bombesin may stimulate proliferation of human pancreatic cancer cells through an

autocrine pathway. *International Journal of Cancer*, 68(4), 528–534.
[https://doi.org/10.1002/\(SICI\)1097-0215\(19961115\)68:4<528::AID-IJC20>3.0.CO;2-#](https://doi.org/10.1002/(SICI)1097-0215(19961115)68:4<528::AID-IJC20>3.0.CO;2-#)

- World Health Organization. (2018). Cancer Fact Sheet. Retrieved from <http://www.who.int/mediacentre/factsheets/fs297/en/>
- Wu, X., Ma, Y., Cheng, J., Li, X., Zheng, H., Jiang, L., & Zhou, R. (2017). TIPE1 function as a prognosis predictor and negative regulator of lung cancer. *Oncotarget*, 8(45), 78496–78506. <https://doi.org/10.18632/oncotarget.19655>
- Xing, B., & Ren, C. (2016). Tumor-suppressive miR-99a inhibits cell proliferation via targeting of TNFAIP8 in osteosarcoma cells. *American Journal of Translational Research*, 8(2), 1082–1090. Retrieved from <http://www.ncbi.nlm.nih.gov/pubmed/27158394>
- Zhang, X., Wang, J., Fan, C., Li, H., Sun, H., Gong, S., ... Shi, Y. (2009). Crystal structure of TIPE2 provides insights into immune homeostasis. *Nature Structural and Molecular Biology*, 16(1), 89–90. <https://doi.org/10.1038/nsmb.1522>
- Zhang, Z., Liang, X., Gao, L., Ma, H., Liu, X., Pan, Y., ... Ma, C. (2015). TIPE1 induces apoptosis by negatively regulating Rac1 activation in hepatocellular carcinoma cells. *Oncogene*, 34(20), 2566–2574. <https://doi.org/10.1038/onc.2014.208>
- Zhang, Z., Qi, H., Hou, S., & Jin, X. (2013). TIPE2 mRNA overexpression correlates with TNM staging in renal cell carcinoma tissues. *Oncology Letters*, 6(2), 571–575. <https://doi.org/10.3892/ol.2013.1388>

APPENDIX A

Supplementary Data



Supplementary Figure 1. Results of mammalian two-hybrid assay. The fusion construct VP16-MyoD + GAL4-Id was used as a positive control. Relative interaction was calculated as a ratio of firefly luciferase activity to *Renilla* luciferase activity. Individual points represent replicates. Controls were performed with 4 replicates each and experimental wells had 8 replicates for each. No significant interaction between experimental constructs was seen in either experiment.

Gene stable ID	Gene start (bp)	Gene end (bp)	Gene description	Chromosome/scaffold name	Gene name
ENSG00000179869	48171458	48647496	ATP binding cassette subfamily A member 13 [Source:HGNC Symbol;Acc:HGNC:14638]	7	ABCA13
ENSG00000073734	168922938	169031322	ATP binding cassette subfamily B member 11 [Source:HGNC Symbol;Acc:HGNC:42]	2	ABCB11
ENSG00000281179	21717808	21718245		15	AC135068.8
ENSG00000127507	14732393	14778541	adhesion G protein-coupled receptor E2 [Source:HGNC Symbol;Acc:HGNC:3337]	19	ADGRE2
ENSG00000205336	57610652	57665580	adhesion G protein-coupled receptor G1 [Source:HGNC Symbol;Acc:HGNC:4512]	16	ADGRG1
ENSG00000053371	19303965	19312146	aldo-keto reductase family 7 member A2 [Source:HGNC Symbol;Acc:HGNC:389]	1	AKR7A2
ENSG00000282988	26195595	26199293		6	AL031777.3
ENSG00000132746	67662162	67681200	aldehyde dehydrogenase 3 family member B2 [Source:HGNC Symbol;Acc:HGNC:411]	11	ALDH3B2
ENSG00000126016	112774503	112840815	angiominin [Source:HGNC Symbol;Acc:HGNC:17810]	X	AMOT
ENSG00000136250	36512949	36724549	acyloxyacyl hydrolase [Source:HGNC Symbol;Acc:HGNC:548]	7	AOAH
ENSG00000107863	24583609	24723668	Rho GTPase activating protein 21 [Source:HGNC Symbol;Acc:HGNC:23725]	10	ARHGAP21
ENSG00000064787	53936777	54070594	breast carcinoma amplified sequence 1 [Source:HGNC Symbol;Acc:HGNC:974]	20	BCAS1
ENSG00000169594	83255903	83284714	basonuclin 1 [Source:HGNC Symbol;Acc:HGNC:1081]	15	BNC1
ENSG00000175573	65916808	65919117	chromosome 11 open reading frame 68 [Source:HGNC Symbol;Acc:HGNC:28801]	11	C11orf68
ENSG00000260220	136249971	136306901	coiled-coil domain containing 187 [Source:HGNC Symbol;Acc:HGNC:30942]	9	CCDC187
ENSG00000140326	42723544	42737128	codanin 1 [Source:HGNC Symbol;Acc:HGNC:1713]	15	CDAN1
ENSG00000130177	114234887	114272723	cell division cycle 16 [Source:HGNC Symbol;Acc:HGNC:1720]	13	CDC16
ENSG00000123219	65517766	65563171	centromere protein K [Source:HGNC Symbol;Acc:HGNC:29479]	5	CENPK
ENSG00000126001	35455164	35519280	centrosomal protein 250 [Source:HGNC Symbol;Acc:HGNC:1859]	20	CEP250
ENSG00000120051	104353764	104455090	cilia and flagella associated protein 58 [Source:HGNC Symbol;Acc:HGNC:26676]	10	CFAP58
ENSG00000164309	79689877	79800240	cardiomyopathy associated 5 [Source:HGNC Symbol;Acc:HGNC:14305]	5	CMYA5
ENSG00000138767	77713387	77819615	CCR4-NOT transcription complex subunit 6 like	4	CNOT6L

ENSG00000165078	67422038	67746385	[Source:HGNC Symbol;Acc:HGNC:18042] carboxypeptidase A6 [Source:HGNC Symbol;Acc:HGNC:17245]	8	CPA6
ENSG00000203710	207496147	207641765	complement C3b/C4b receptor 1 (Knops blood group) [Source:HGNC Symbol;Acc:HGNC:2334]	1	CR1
ENSG00000142544	51097606	51108370	cytosolic thiouridylase subunit 1 [Source:HGNC Symbol;Acc:HGNC:29590]	19	CTU1
ENSG00000139990	69050881	69153150	DDB1 and CUL4 associated factor 5 [Source:HGNC Symbol;Acc:HGNC:20224]	14	DCAF5
ENSG00000156136	70992538	71030914	deoxycytidine kinase [Source:HGNC Symbol;Acc:HGNC:2704]	4	DCK
ENSG00000177030	644233	706715	DEAF1, transcription factor [Source:HGNC Symbol;Acc:HGNC:14677]	11	DEAF1
ENSG00000163214	38797729	38875934	DExH-box helicase 57 [Source:HGNC Symbol;Acc:HGNC:20086]	2	DHX57
ENSG00000116544	34865436	34929585	DLG associated protein 3 [Source:HGNC Symbol;Acc:HGNC:30368]	1	DLGAP3
ENSG00000007174	11598431	11969748	dynein axonemal heavy chain 9 [Source:HGNC Symbol;Acc:HGNC:2953]	17	DNAH9
ENSG00000128512	111726110	112206411	dedicator of cytokinesis 4 [Source:HGNC Symbol;Acc:HGNC:19192]	7	DOCK4
ENSG00000088387	98793429	99086625	dedicator of cytokinesis 9 [Source:HGNC Symbol;Acc:HGNC:14132]	13	DOCK9
ENSG00000113719	172834275	172952685	endoplasmic reticulum-golgi intermediate compartment 1 [Source:HGNC Symbol;Acc:HGNC:29205]	5	ERGIC1
ENSG00000070367	57200507	57269008	exocyst complex component 5 [Source:HGNC Symbol;Acc:HGNC:10696]	14	EXOC5
ENSG00000174137	1617915	1684302	family with sequence similarity 53 member A [Source:HGNC Symbol;Acc:HGNC:31860]	4	FAM53A
ENSG00000116120	222570536	222656337	phenylalanyl-tRNA synthetase beta subunit [Source:HGNC Symbol;Acc:HGNC:17800]	2	FARSB
ENSG00000196159	125316399	125492932	FAT atypical cadherin 4 [Source:HGNC Symbol;Acc:HGNC:23109]	4	FAT4
ENSG00000007933	171090877	171117819	flavin containing monooxygenase 3 [Source:HGNC Symbol;Acc:HGNC:3771]	1	FMO3
ENSG00000113327	162000057	162162977	gamma-aminobutyric acid type A receptor gamma2 subunit [Source:HGNC Symbol;Acc:HGNC:4087]	5	GABRG2
ENSG00000154252	241776825	241804208	galactose-3-O- sulfotransferase 2 [Source:HGNC Symbol;Acc:HGNC:24869]	2	GAL3ST2
ENSG00000276126	241799063	241804208	galactose-3-O- sulfotransferase 2 [Source:HGNC Symbol;Acc:HGNC:24869]		CHR_HSCHR2_3_CTG15 GAL3ST2

ENSG00000155511	153489615	153813869	glutamate ionotropic receptor AMPA type subunit 1 [Source:HGNC Symbol;Acc:HGNC:4571]	5	GRIA1
ENSG00000120251	157204182	157366075	glutamate ionotropic receptor AMPA type subunit 2 [Source:HGNC Symbol;Acc:HGNC:4572]	4	GRIA2
ENSG00000125675	123184153	123490915	glutamate ionotropic receptor AMPA type subunit 3 [Source:HGNC Symbol;Acc:HGNC:4573]	X	GRIA3
ENSG00000152578	105609994	105982092	glutamate ionotropic receptor AMPA type subunit 4 [Source:HGNC Symbol;Acc:HGNC:4574]	11	GRIA4
ENSG00000187166	48328980	48330279	H1 histone family member N, testis specific [Source:HGNC Symbol;Acc:HGNC:24893]	12	H1FNT
ENSG00000246705	14774383	14778002	H2A histone family member J [Source:HGNC Symbol;Acc:HGNC:14456]	12	H2AFJ
ENSG00000105968	44826791	44848083	H2A histone family member V [Source:HGNC Symbol;Acc:HGNC:20664]	7	H2AFV
ENSG00000188486	119093854	119095467	H2A histone family member X [Source:HGNC Symbol;Acc:HGNC:4739]	11	H2AFX
ENSG00000164032	99948086	99950388	H2A histone family member Z [Source:HGNC Symbol;Acc:HGNC:4741]	4	H2AFZ
ENSG00000164508	25726132	25726527	histone cluster 1 H2A family member a [Source:HGNC Symbol;Acc:HGNC:18729]	6	HIST1H2AA
ENSG00000278463	26033176	26033568	histone cluster 1 H2A family member b [Source:HGNC Symbol;Acc:HGNC:4734]	6	HIST1H2AB
ENSG00000180573	26124145	26139116	histone cluster 1 H2A family member c [Source:HGNC Symbol;Acc:HGNC:4733]	6	HIST1H2AC
ENSG00000196866	26198851	26199243	histone cluster 1 H2A family member d [Source:HGNC Symbol;Acc:HGNC:4729]	6	HIST1H2AD
ENSG00000277075	26216975	26217483	histone cluster 1 H2A family member e [Source:HGNC Symbol;Acc:HGNC:4724]	6	HIST1H2AE
ENSG00000196787	27133042	27135291	histone cluster 1 H2A family member g [Source:HGNC Symbol;Acc:HGNC:4737]	6	HIST1H2AG
ENSG00000274997	27147129	27147515	histone cluster 1 H2A family member h [Source:HGNC Symbol;Acc:HGNC:13671]	6	HIST1H2AH
ENSG00000196747	27808199	27808701	histone cluster 1 H2A family member i [Source:HGNC Symbol;Acc:HGNC:4725]	6	HIST1H2AI
ENSG00000276368	27814354	27814740	histone cluster 1 H2A family member j [Source:HGNC Symbol;Acc:HGNC:4727]	6	HIST1H2AJ
ENSG00000275221	27837947	27838339	histone cluster 1 H2A family member k [Source:HGNC Symbol;Acc:HGNC:4726]	6	HIST1H2AK
ENSG00000276903	27865355	27865747	histone cluster 1 H2A family member l [Source:HGNC Symbol;Acc:HGNC:4730]	6	HIST1H2AL
ENSG00000278677	27892757	27893149	histone cluster 1 H2A family member m [Source:HGNC Symbol;Acc:HGNC:4735]	6	HIST1H2AM
ENSG00000203812	149842188	149842736	histone cluster 2 H2A family member a3 [Source:HGNC	1	HIST2H2AA3

ENSG00000272196	149851061	149851624	Symbol;Acc:HGNC:4736] histone cluster 2 H2A family member a4 [Source:HGNC Symbol;Acc:HGNC:29668]	1	HIST2H2AA4
ENSG00000184260	149886975	149887364	histone cluster 2 H2A family member c [Source:HGNC Symbol;Acc:HGNC:4738]	1	HIST2H2AC
ENSG00000181218	228456979	228457873	histone cluster 3 H2A [Source:HGNC Symbol;Acc:HGNC:20507]	1	HIST3H2A
ENSG00000135486	54280193	54287088	heterogeneous nuclear ribonucleoprotein A1 [Source:HGNC Symbol;Acc:HGNC:5031]	12	HNRNPA1
ENSG00000163913	129440036	129520507	intraflagellar transport 122 [Source:HGNC Symbol;Acc:HGNC:13556]	3	IFT122
ENSG00000270505	22160431	22160868	immunoglobulin heavy variable 1/OR15-1 (non- functional) [Source:HGNC Symbol;Acc:HGNC:5563]	15	IGHV1OR15- 1
ENSG00000270467	33802764	33803217	immunoglobulin heavy variable 3/OR16-12 (non- functional) [Source:HGNC Symbol;Acc:HGNC:5636]	16	IGHV3OR16- 12
ENSG00000149503	62123973	62153163	inner centromere protein [Source:HGNC Symbol;Acc:HGNC:6058]	11	INCENP
ENSG00000188487	15112424	15247208	INSC, spindle orientation adaptor protein [Source:HGNC Symbol;Acc:HGNC:33116]	11	INSC
ENSG00000168264	234604269	234609525	interferon regulatory factor 2 binding protein 2 [Source:HGNC Symbol;Acc:HGNC:21729]	1	IRF2BP2
ENSG00000276289	7816675	7829926	potassium voltage-gated channel subfamily E regulatory subunit 1B [Source:HGNC Symbol;Acc:HGNC:52280]	21	KCNE1B
ENSG00000197705	32672671	32773062	kelch like family member 14 [Source:HGNC Symbol;Acc:HGNC:29266]	18	KLHL14
ENSG00000055609	152134922	152436005	lysine methyltransferase 2C [Source:HGNC Symbol;Acc:HGNC:13726]	7	KMT2C
ENSG00000135480	52232520	52252186	keratin 7 [Source:HGNC Symbol;Acc:HGNC:6445]	12	KRT7
ENSG00000141068	27456470	27626438	kinase suppressor of ras 1 [Source:HGNC Symbol;Acc:HGNC:6465]	17	KSR1
ENSG00000133067	202193901	202319781	leucine rich repeat containing G protein- coupled receptor 6 [Source:HGNC Symbol;Acc:HGNC:19719]	1	LGR6
ENSG00000167210	46476972	46657220	lipoxygenase homology domains 1 [Source:HGNC Symbol;Acc:HGNC:26521]	18	LOXHD1
ENSG00000147381	151912509	151925170	MAGE family member A4 [Source:HGNC Symbol;Acc:HGNC:6802]	X	MAGEA4
ENSG00000196547	90902218	90922584	mannosidase alpha class 2A member 2 [Source:HGNC Symbol;Acc:HGNC:6825]	15	MAN2A2
ENSG00000168906	85539165	85545280	methionine adenosyltransferase 2A [Source:HGNC Symbol;Acc:HGNC:6904]	2	MAT2A

ENSG00000258839	89912119	89920977	melanocortin 1 receptor [Source:HGNC Symbol;Acc:HGNC:6929]	16	MC1R
ENSG00000183019	7676628	7679826	mast cell expressed membrane protein 1 [Source:HGNC Symbol;Acc:HGNC:27291]	19	MCEMP1
ENSG00000175221	867630	893218	mediator complex subunit 16 [Source:HGNC Symbol;Acc:HGNC:17556]	19	MED16
ENSG00000176624	51174550	51218304	mex-3 RNA binding family member C [Source:HGNC Symbol;Acc:HGNC:28040]	18	MEX3C
ENSG00000135517	56449502	56469166	major intrinsic protein of lens fiber [Source:HGNC Symbol;Acc:HGNC:7103]	12	MIP
ENSG00000171843	20341665	20622543	MLLT3, super elongation complex subunit [Source:HGNC Symbol;Acc:HGNC:7136]	9	MLLT3
ENSG00000074071	1771890	1773155	mitochondrial ribosomal protein S34 [Source:HGNC Symbol;Acc:HGNC:16618]	16	MRPS34
ENSG00000197535	52307283	52529050	myosin VA [Source:HGNC Symbol;Acc:HGNC:7602]	15	MYO5A
ENSG00000066248	232878686	233013272	neuronal guanine nucleotide exchange factor [Source:HGNC Symbol;Acc:HGNC:7807]	2	NGEF
ENSG00000055044	202265716	202303666	NOP58 ribonucleoprotein [Source:HGNC Symbol;Acc:HGNC:29926]	2	NOP58
ENSG00000170485	100820152	100996829	neuronal PAS domain protein 2 [Source:HGNC Symbol;Acc:HGNC:7895]	2	NPAS2
ENSG00000148200	124517275	124771310	nuclear receptor subfamily 6 group A member 1 [Source:HGNC Symbol;Acc:HGNC:7985]	9	NR6A1
ENSG00000122126	129539849	129592561	OCRL, inositol polyphosphate-5- phosphatase [Source:HGNC Symbol;Acc:HGNC:8108]	X	OCRL
ENSG00000167332	4680171	4697854	olfactory receptor family 51 subfamily E member 2 [Source:HGNC Symbol;Acc:HGNC:15195]	11	OR51E2
ENSG00000172464	56641466	56642471	olfactory receptor family 5 subfamily AP member 2 [Source:HGNC Symbol;Acc:HGNC:15258]	11	OR5AP2
ENSG00000181752	56159394	56160317	olfactory receptor family 8 subfamily K member 5 [Source:HGNC Symbol;Acc:HGNC:15315]	11	OR8K5
ENSG00000187950	29412474	29497686	ovochymase 1 [Source:HGNC Symbol;Acc:HGNC:23080]	12	OVCH1
ENSG00000110811	6828410	6839851	prolyl 3-hydroxylase 3 [Source:HGNC Symbol;Acc:HGNC:19318]	12	P3H3
ENSG00000163110	94451857	94668227	PDZ and LIM domain 5 [Source:HGNC Symbol;Acc:HGNC:17468]	4	PDLIM5
ENSG00000185238	20387530	20509294	protein arginine methyltransferase 3 [Source:HGNC Symbol;Acc:HGNC:30163]	11	PRMT3
ENSG00000135406	49293252	49298686	peripherin [Source:HGNC Symbol;Acc:HGNC:9461]	12	PRPH

ENSG00000100804	23016543	23035230	proteasome subunit beta 5 [Source:HGNC Symbol;Acc:HGNC:9542]	14	PSMB5
ENSG00000108469	75626845	75667189	RecQ like helicase 5 [Source:HGNC Symbol;Acc:HGNC:9950]	17	RECQL5
ENSG00000143344	183636085	183928531	ral guanine nucleotide dissociation stimulator like 1 [Source:HGNC Symbol;Acc:HGNC:30281]	1	RGL1
ENSG00000080345	151409883	151508013	replication timing regulatory factor 1 [Source:HGNC Symbol;Acc:HGNC:23207]	2	RIF1
ENSG00000137522	71928701	71997597	ring finger protein 121 [Source:HGNC Symbol;Acc:HGNC:21070]	11	RNF121
ENSG00000198863	42980565	42993690	RUN domain containing 1 [Source:HGNC Symbol;Acc:HGNC:25418]	17	RUNDC1
ENSG00000196218	38433699	38587564	ryanodine receptor 1 [Source:HGNC Symbol;Acc:HGNC:10483]	19	RYR1
ENSG00000137872	47184101	47774223	semaphorin 6D [Source:HGNC Symbol;Acc:HGNC:16770]	15	SEMA6D
ENSG00000163904	185582496	185633551	SUMO1/sentrin/SMT3 specific peptidase 2 [Source:HGNC Symbol;Acc:HGNC:23116]	3	SEN2
ENSG00000140264	43777087	43802589	small EDRK-rich factor 2 [Source:HGNC Symbol;Acc:HGNC:10757]	15	SERF2
ENSG00000170364	4303304	4317567	SET domain and mariner transposase fusion gene [Source:HGNC Symbol;Acc:HGNC:10762]	3	SETMAR
ENSG00000100014	24270817	24417740	sperm antigen with calponin homology and coiled-coil domains 1 like [Source:HGNC Symbol;Acc:HGNC:29022]	22	SPECC1L
ENSG00000138600	50702266	50765808	signal peptide peptidase like 2A [Source:HGNC Symbol;Acc:HGNC:30227]	15	SPPL2A
ENSG00000159433	42575659	42720981	StAR related lipid transfer domain containing 9 [Source:HGNC Symbol;Acc:HGNC:19162]	15	STARD9
ENSG00000164506	147204425	147390476	syntaxin binding protein 5 [Source:HGNC Symbol;Acc:HGNC:19665]	6	STXBP5
ENSG00000144455	3700814	4467281	sulfatase modifying factor 1 [Source:HGNC Symbol;Acc:HGNC:20376]	3	SUMF1
ENSG00000156787	123041968	123152153	TBC1 domain family member 31 [Source:HGNC Symbol;Acc:HGNC:30888]	8	TBC1D31
ENSG00000176946	241584405	241637449	THAP domain containing 4 [Source:HGNC Symbol;Acc:HGNC:23187]	2	THAP4
ENSG00000115705	1374223	1543711	thyroid peroxidase [Source:HGNC Symbol;Acc:HGNC:12015]	2	TPO
ENSG00000277603	1372594	1540021	thyroid peroxidase [Source:HGNC Symbol;Acc:HGNC:12015]	CHR_HSCHR2_4_CTG1	TPO
ENSG00000128881	42738734	42920809	tau tubulin kinase 2 [Source:HGNC Symbol;Acc:HGNC:19141]	15	TTBK2
ENSG00000177398	42062959	42143453	uromodulin like 1	21	UMODL1

ENSG00000109189	52590972	52659335	[Source:HGNC Symbol;Acc:HGNC:12560] ubiquitin specific peptidase 46 [Source:HGNC Symbol;Acc:HGNC:20075]	4	USP46
ENSG00000143952	63892146	64019072	VPS54, GARP complex subunit [Source:HGNC Symbol;Acc:HGNC:18652]	2	VPS54
ENSG00000167716	1716523	1738599	WD repeat domain 81 [Source:HGNC Symbol;Acc:HGNC:26600]	17	WDR81
ENSG00000276021	1716523	1738610	WD repeat domain 81 [Source:HGNC Symbol;Acc:HGNC:26600]	CHR_HSCHR17_1_CTG2	WDR81
ENSG00000142784	27234516	27308633	WD and tetratricopeptide repeats 1 [Source:HGNC Symbol;Acc:HGNC:29175]	1	WDTC1
ENSG00000241127	39566376	39610320	Yae1 domain containing 1 [Source:HGNC Symbol;Acc:HGNC:24857]	7	YAE1D1
ENSG00000140836	72782885	73891871	zinc finger homeobox 3 [Source:HGNC Symbol;Acc:HGNC:777]	16	ZFHX3
ENSG00000196646	12163064	12189881	zinc finger protein 136 [Source:HGNC Symbol;Acc:HGNC:12920]	19	ZNF136
ENSG00000267680	44094339	44109886	zinc finger protein 224 [Source:HGNC Symbol;Acc:HGNC:13017]	19	ZNF224
ENSG00000160094	33256545	33300719	zinc finger protein 362 [Source:HGNC Symbol;Acc:HGNC:18079]	1	ZNF362
ENSG00000180938	124973298	124979389	zinc finger protein 572 [Source:HGNC Symbol;Acc:HGNC:26758]	8	ZNF572
ENSG00000188171	20620061	20661596	zinc finger protein 626 [Source:HGNC Symbol;Acc:HGNC:30461]	19	ZNF626

Supplementary Table 1. Summary of 138 unique genes interactors pulled out in mass spectrometry.

AUTHOR'S BIOGRAPHY

Audrey V. Hoyle was born in Norway, Maine on December 31, 1994. She was raised in Alfred, Maine with her three siblings and graduated from Massabesic High School in 2013. Upon completion of a dual degree program, Audrey will hold bachelor's degrees in biochemistry and microbiology. She is a member of Phi Beta Kappa and the National Society of Collegiate Scholars. She is co-founder and co-president of the Vegan Education and Empowerment Coalition at the University of Maine, and an Emergency Medical Technician at the University Volunteer Ambulance Corps. She works as a teaching assistant in the general microbiology lab and microbiology lab for the professional nurse.

Upon graduation, Audrey plans to work as an EMT and travel before attending medical school to pursue a career in emergency medicine. She plans on volunteering her services to Doctors without Borders.